University of Zurich[UZH]

USZ Universitäts Spital Zürich

Volume de-escalated radiotherapy for head and neck cancer: A TCP and NTCP based optimization approach

Master thesis in physics

Muriel Baldinger

June 2024

Supervisor: Prof. Dr. Jan Unkelbach
Tutor: Yoel Pérez Haas

Physik Institut, University of Zurich
Department of Radiation Oncology, University Hospital Zürich, Switzerland

Abstract

This thesis focuses on optimizing treatment plans for oropharyngeal squamous cell carcinoma (OSCC) patients by improving the balance between tumor control probability (TCP) and normal tissue complication probability (NTCP). The study is divided into two parts: volume de-escalation of treatment plans and the incorporation of a TCP model into the treatment planning process.

In the first part, we develop and evaluate volume de-escalated treatment plans that reduce the elective target volume, based on a lymphatic progression model. The greatest dose reduction is achieved further down the neck by avoiding the irradiation of lymph node levels IV and V.

The second part of the thesis integrates a voxel based TCP model, which considers the probability of tumor involvement in different lymph node levels, into the treatment planning process. By integrating the TCP into the calculation of optimal dose distributions, we demonstrate the potential to reduce the total dose delivered to organs at risk (OAR) while maintaining high TCP. This is achieved by lowering the dose near the OAR and applying a higher dose in the remaining LNL. This approach ensures high TCP values and reduces NTCP values, thereby lowering the likelihood of complications.

Contents

1 Introduction **1**

2 Context and problem **2**
2.1 Radiotherapy . . . 2
2.2 Head and neck cancer . . . 3
2.3 Intensity modulated radiotherapy . . . 4
2.3.1 Plan optimization . . . 5
2.3.2 Gradient descent . . . 6
2.4 Lymphatic progression model . . . 6

3 Comparing standard care with volume de-escalate treatment plans **8**
3.1 Normal tissue complication probability . . . 8
3.1.1 Xerostomia and sticky saliva . . . 8
3.1.2 Swallowing problems . . . 9
3.1.3 Hypothroidism . . . 10
3.2 Data preparation . . . 11
3.3 NTCP calculation and plan comparison . . . 13

4 Tumor control probability **16**
4.1 Probabilistic clinical target volume concept . . . 18
4.2 Probabilistic TCP . . . 19
4.2.1 Least square fit . . . 20
4.3 Validation of TCP_q . . . 22

5 Implementation of a treatment plan optimization **24**
5.1 A computational environment for radiotherapy research . . . 24
5.2 Interior point optimizer . . . 24
5.3 Quadratic objective . . . 24
5.4 Falloff objective . . . 26
5.5 Mean dose objective . . . 27
5.5.1 NTCP for pharyngeal constrictor muscle . . . 28
5.5.2 Implementation mean dose objective . . . 28
5.6 Tumor control probability objective . . . 29
5.7 Results . . . 32
5.7.1 Patient 2 . . . 32
5.7.2 Patient 1 . . . 34
5.7.3 Patient 8 . . . 36

6 Discussion **39**
6.1 Comparing standard care with volume de-escalate treatment plans . . . 39
6.2 Implementation of a treatment plan optimization . . . 39

7 Conclusion and Outlook **41**

8 Acknowledgement **42**

1 Introduction

Treating cancer remains a challenge in modern medicine. One of the primary challenges in radiotherapy is to maximize tumor control while minimizing damage to surrounding healthy tissues. With less damage to the healthy tissue, the patient will experience less side effects. [1]
Radiotherapy has evolved significantly over the past few decades, with Intensity Modulated Radiotherapy (IMRT) emerging as a revolutionary technique. IMRT allows for the delivery of highly conformal radiation doses to complex-shaped tumor volumes, thereby sparing surrounding normal tissues to a much greater extent than conventional radiotherapy techniques. This improvement has led to better dose distributions and better outcomes. [2]
Among the various types of cancer, head and neck cancers are particularly difficult to treat due to their impact on essential functions such as speech, swallowing, and breathing. Despite the use of IMRT the treatment of head and neck cancer presents significant challenges. The anatomical complexity and proximity of critical structures in the head and neck region require exact planning. The definition of the target volume in head and neck cancer patients is a topic of ongoing debate among experts. The tumor can spread into the lymphatic system and form metastases, often not detectable on the medical images. Increasing the irradiated volume raises the likelihood of killing all the tumor cells but also the risk of different side effects. [1, 3]
An effective way to understand the quality of a treatment plan is through the tumor control probability (TCP) and the normal tissue complication probability (NTCP). The TCP models aim to predict the probability of achieving local tumor control based on the radiation dose delivered to the target, while the NTCP models predict the probability of experiencing side effects based on the dose distribution. A good treatment plan maximizes TCP and minimizes NTCP. [1]
The first part of this thesis compares standard of care treatment plans with volume de-escalate plans, where smaller target volumes were defined, for oropharyngeal cancer patients. To compare the two plans, NTCP models were used, to better understand the impact of dose reduction on side effects.
In the second part, the thesis focuses on the development and implementation of a TCP model for electively irradiated LNLs to optimize IMRT treatment plans for oropharyngeal cancer patients. The goal is to calculate treatment plans that are optimized based on a TCP model but also consider one or more NTCP models. In the end, a trade-off between controlling the tumor and sparing the healthy tissue should be reached for an optimal treatment of the patient.

2 Context and problem

This chapter, introduces the basics of radiotherapy and the most common radiation techniques that are applied. Additionally, head and neck cancer will be briefly discussed to provide context for this work. To de-escalate the radiotherapy, a mathematical lymphatic spread model was applied, which was developed by the research group. A brief description of this model and its application in volume de-escalating treatments is also provided in this chapter.

2.1 Radiotherapy

Radiotherapy is one of the most common treatments for cancer. Half of all cancer patients receive radiotherapy during their treatment. Other treatment modalities for tumors include surgery and chemotherapy, with many cases involving a combination of at least two modalities. [1]
Radiotherapy uses ionizing radiation to destroy tumor cells. The most common type of radiation used are photons. The photons are produced in a linear accelerator (LINAC) with an energy ranging from 4 to 25 MV depending on the treatment. After acceleration, the photons have enough energy to lead to ionizations within the cells of the patient. In this energy range, the photons primarily interact with matter through the Compton effect. Due to this interaction, electrons are ejected inside the patient. The ejected electrons will induce damage to the surrounding tissue. Due to their charge there are more interactions with the tissue which leads to more ionization and therefore to more damage. [1]
The goal of radiotherapy is to destroy tumor tissue. It is achieved by causing ionization within the tumor cells, which leads to cellular damage. However, ionization can also occur in the surrounding healthy tissue, posing a challenge in treatment. Ionization induces various types of lesions in the cell, which can ultimately result in cell death. A critical type of lesion is the double strand break in the DNA. When such a break occurs, the DNA cannot repair itself, leading to the death of the cell. [1]
Before irradiating a patient, one needs to define the tumor volume. To detect and define tumor tissue, different imaging modalities are applied. The most common modalities encompass Computer Tomography (CT), Magnetic Resonance Imaging (MRI), Ultrasound and Positron Emission Tomography (PET). For radiotherapy CT images are essential, as these images provide density information for radiation dose calculations. [3]
However, CT images alone are not sufficient to setup a radiotherapy plan. Since the soft tissue contrast in CT images is inferior to other imaging modalities, it is not optimal to outline tumors based solely on CT images. To compensate, MR images are acquired, which have better soft tissue contrast. A further improvement in tumor tissue detection can be achieved with PET imaging. The combination of all imaging modalities provide good information for treatment planning. [3]
After the images have been acquired, the tumor and the organs at risk (OAR) are contoured. The target volume is split up in three parts. The gross tumor volume (GTV) (see figure 1) comprises the central volume defined by clinical examination or by imaging. The GTV is extended to the clinical target volume (CTV), which should contain the microscopic spread of the tumor. The size of the CTV is defined on prior knowledge and anatomical boundaries. The last extension is the planning target volume (PTV). The PTV accounts for patient movement and internal organs shifting. The OARs have an important role in radiotherapy planning. Too much dose can lead to side effects which impact the quality of life of the patient after treatment. Different organs have different tolerances and dose limits which need to be accounted. If, for example, one delivers too much dose to the spinal cord, the patient could be permanently paralyzed. [3]

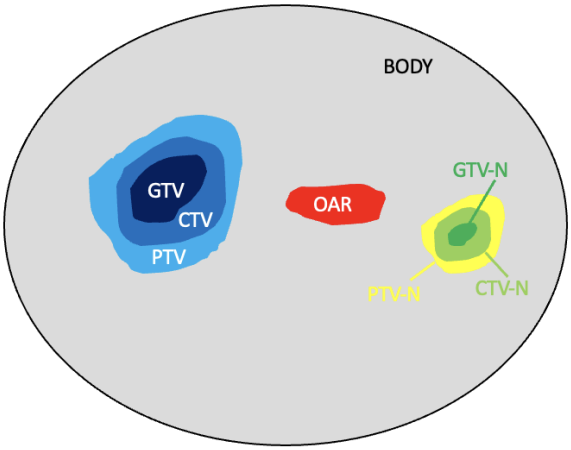

Figure 1: Schematic figure depicting a hypothetical patient geometry. On the left side, the target volumes for the primary tumor are drawn. In red, an organ at risk is shown. On the right side the target volumes for a metastasis are outlined.

2.2 Head and neck cancer

Due to the proximity of many organs in the head and neck area, the treatment is difficult, and many side effects can not be avoided. Head and neck tumors can impair the speech or food intake. The treatment of head and neck cancer consist of surgery, (chemo)radiotherapy, or a combination of both. [3]
Due to the lymphatic drainage system, metastases in the lymph nodes are very common. In radiotherapy, the target volume not only contains the primary target volume, but also the clinically detected lymph node metastases. The macroscopic metastases are contoured as nodal gross tumor volume (GTV-N) (see figure 1). To account for the microscopic spread in the lymphatic system, which is not visible on imaging modalities, the elective clinical target volume (CTV-N) is defined. This extension should contain all the parts of the lymph drainage system that are at risk of harboring occult metastases. To better define the CTV-N the lymphatic system is divided in different lymph node levels (LNL) like in figure 2. [3]

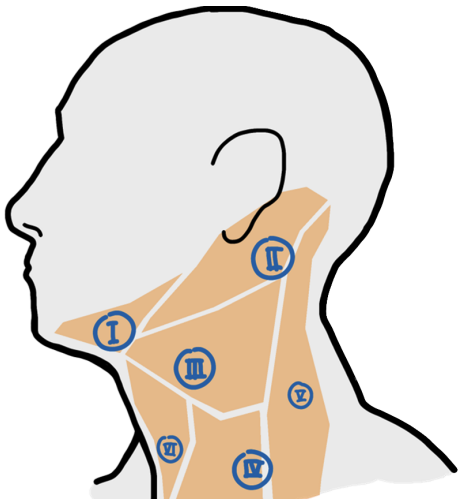

Figure 2: Schematic figure depicting the division of the lymphatic system in the head and neck region in different lymph node levels [4].

Additionally, the head of a patient is divided in an ipsilateral side (ipsi) and a contralateral side (contra). The ipsilateral side is the side of the head from where the tumor originated. The

contralateral side is the opposite side from where the tumor started growing. [3]
The elective CTV is currently based on clinical recommendations [5]. The nodal planning target volume (PTV-N) is the extension of the CTV-N to account for motion. We specifically look at oropharyngeal cancer, which is a specific subside of head and neck cancer.

2.3 Intensity modulated radiotherapy

IMRT is considered a standard treatment for head and neck cancers. It allows irradiating concave target volumes by being able to deliver inhomogeneous fluence distributions across the treatment field. Concave target volumes allow better OAR sparing. Thus, the prescribed dose can be increased without damaging the organs at risk. Additionally, with IMRT it is possible to deliver different dose levels to different regions of the tumor. For these things to be possible, the patient is divided into small volumes called voxels, which are like three-dimensional pixels. [2]
IMRT involves modulating the fluence distribution of radiation beams perpendicular to the incident beam direction. This modulation is achieved by dividing the radiation beam into small segments. These segments, known as beamlets or bixels, discretize the lateral fluence distribution of the beam. A beamlet can have different sizes depending on the treatment machine. The discrete representation of the fluence is called the fluence map. [2]
IMRT planning aims to determine fluence maps for all incident beam directions to achieve the best possible dose distribution in the patient. This optimization problem, called Fluence Map Optimization (FMO), involves selecting all potentially beneficial beamlets contributing significant dose to the target volume. In figure 3 all the beamlets are marked green that would contribute to the pink target. For each beam angle different beamlets are selected. [2]

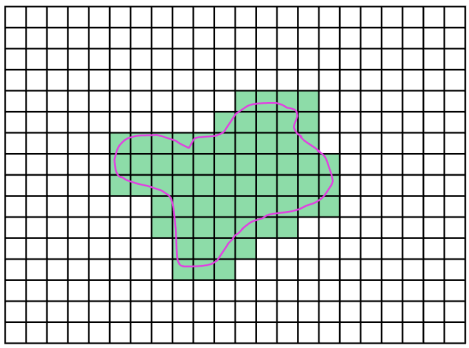

Figure 3: Schematic figure of selected beamlets (green) that could contribute dose to the target volume (pink).

To evaluate the quality of a treatment plan the dose distribution is examined to check whether the goals are reached. For example, the whole target should receive a conformal dose. The maximum dose limits for OAR should not be exceeded, else the patient could experience permanent damage. A dose falloff around the target should be visible, the steeper, the better. In a commercial treatment planning system we can additionally check the clinical goals from the clinician. [2]
To visualize the planned dose distribution in radiotherapy, we need to approximate the fluence maps from all beam directions. The fluence map represents the intensity of the radiation beams as they pass through the patient. To understand how this fluence translates into the actual dose distribution within the patient, we use a tool called the dose-deposition matrix. A dose calculation algorithm calculates the dose distribution of each beamlet in the fluence map within the patient. Denoting the dose contributed by beamlet j to voxel i as D_{ij}, the dose-deposition matrix. The intensity of beamlet j is given by x_j. To find the dose in voxel i one can sum up all the contribution to voxel i:

$$d_i = \sum_j D_{ij} * x_j \tag{1}$$

In IMRT planning, the dose-deposition matrix is typically pre-calculated and stored in memory. [2]

2.3.1 Plan optimization

In IMRT we want to find a well suited fluence map. To do so, we need to mathematically define what an optimal fluence map is and with that what our desired dose distribution should look like. The prescribed dose for each target volume defines the goal to be reached, while the dose to the target should be delivered as homogeneous as possible. If less dose is delivered, then the tumor could persist, but if more dose than prescribed is delivered, then the patient can be subject to unnecessary harm. [2]
The dose delivered should only be applied to the target volume. Generally, this is not possible, else the homogeneous dose to the tumor gets jeopardized. The compromise is the steepest falloff possible around the target volume. While we still aim for a uniform dose distribution to the target, the falloff avoids unnecessary dose to the healthy tissue. [2]
The healthy tissue not only gets spared with a falloff, we also try to minimize the dose to the OAR in general. By minimizing the dose, we want to avoid side effects. There are certain organs that have a maximum dose tolerances. If the tolerance is exceeded, severe side effects are the consequence. [2]
To optimize an IMRT plan these goals have to be translated into mathematical terms. They can be stated in equations which then can be used to quantify the quality of a treatment plan. These equations can be split into objectives and constraints. Objective functions evaluate how well a treatment plan aligns with the desired therapeutic goals. The smaller the sum of objecitve is the better the treatment plan fulfills the set goals. To minimize the objectives, the beam intensity in each beamlet can be changed. Constraints are boundaries that can not be exceeded. If the constraints are not met, the treatment plan can not be accepted. These constraints are often used to set maximum or minimum dose tolerances of organ at risks to minimize side effects. [2]
During treatment plan optimization, we aim to minimize all the objectives ($f(d)$) while still respecting the constraints ($g(d)$).

$$\begin{aligned} &\text{minimize} \quad f(d) \\ &\text{subject to} \quad g(d) \leq c \\ &\quad d_i = \sum_j D_{ij} * x_j \\ &\quad x_j \geq 0 \end{aligned} \tag{2}$$

The dose is defined with the dose-deposition matrix multiplied with the beamlet weights. In addition, all the beamlet weights have to be positive ($x_j \geq 0$), because one can not deliver negative dose. [2]
Since there is always dose delivered to the normal tissue, objectives which aim on sparing normal tissue are in conflict with objectives that aim on maximizing tumor dose.Thus, during treatment planning one needs to evaluate the trade-offs By assigning weights w on the objectives based on their importance. A larger weight will make an objective more influential than others. [2]
To find an optimal dose distribution, IMRT uses mathematical optimization algorithms to determine the fluence map x, corresponding to the dose distribution defined in equation 1. The optimization minimizes the weighted sum of the objectives, while complying with all constraints. A common optimization algorithm called gradient descent will be introduced in the next chapter. [2]

2.3.2 Gradient descent

As discussed in equation 2, we can formulate an FMO problem as a mathematical optimization problem. The goal is to minimize the objectives $f(d)$, subject to the constraint $g(d)$. To solve the optimization problem analytically is not possible. The problem is non-convex, which makes finding the global minimum more complex. Additionally, balancing multiple objectives and constraints is very challenging. To evade these problems different optimization algorithms can be used. A common solution is the gradient descent method. [2]
To minimize the sum of objectives with gradient descent, we compute the gradient of each individual objective with respect to the beamlet intensity (x_j). Since the gradient always points into the direction of the steepest increase of a function, one can minimize the objectives by moving in the negative direction of the gradient. Gradient descent is an iterative algorithm, where in each iteration the gradient (∇f) of the actual objective is computed (eq. 3). In each iteration k, a step into the direction of the steepest decrease is taken, updating the intensity of each beamlet. After updating the beamlet weights, the fluence map x is recomputed to calculate the new objective value. The step size (α) needs to be chosen adequately to converge to a reasonable solution. Too large step sizes may prevent finding a local optimum. For too small α the optimization may take too long to find an optimal solution. [2]

$$x^{k+1} = x^k - \alpha * \nabla f \tag{3}$$

Finding the gradient of an objective can be quite difficult. But if the chain rule is applied correctly (eq. 4), the gradient calculations can be simplified. [2]

$$\frac{\partial f}{\partial x_j} = \sum_{i=1}^{N} \frac{\partial f}{\partial d_i} \frac{\partial d_i}{\partial x_j} \tag{4}$$

This can be further simplified. From the definition of the dose deposition matrix (eq. 1) we know that:

$$\frac{\partial d_i}{\partial x_j} = \frac{\partial}{\partial x_j}(\sum_j D_{ij} * x_j) = D_{ij} \tag{5}$$

This equals the dose-fluence matrix which can be calculated before the optimization. This will make the gradient calculations for complex objective a lot simpler. [2]
This basic optimization algorithm has some weaknesses, mainly the slow convergence for IMRT optimizations [2]. But it is enough to understand the basic concept of treatment plan optimization for the later work. We now go on to the model that predicts the volume de-escalate plans.

2.4 Lymphatic progression model

The lymphatic progression model by Ludwig et al. aims to predict the probability of occult metastases in different lymph node levels for oropharyngeal squamous cell carcinoma. With the predictions we hope to minimize the elective target volume and spare healthy tissue. By assigning risk of involvement to LNLs, the model can be used to assess which LNLs should be added to the elective target volume. [4] The model provides a probability of occult metastasis in each LNL given a patient specific diagnosis. Each LNL is described by a binary random variable, which indicates whether the LNL is healthy or involved. Further, each LNL has an observed state, which is another random variable that indicates if the LNL is clinically involved (see figure 4). This information is collected in the diagnosis (D). The diagnosis is connected to the LNL and the tumor with the specificity (S_P) and the sensitivity (S_N). Given that imaging modalities do not have a sensitivity of 1, the model tries to predict the probability of the tumor spreading to any LNL from this information. To model lymphatic spread, a bayesian network is established which depicts the lymphatic system (see figure 4). Where the arcs show all the possible paths the tumor can spread, based on the anatomy of the lymphatic drainage system.The tumor is

connected to each LNL with an arc. Each arc gets assigned a spread probability (b_i), which depicts the probability of spread from the tumor to the connected LNL. Additionally the LNL are connected among themselves and metastasis can spread between the levels. The spread among the levels (t_i) and the spread from the tumor (b_i) are parameters that the model learns. [4, 6–8]

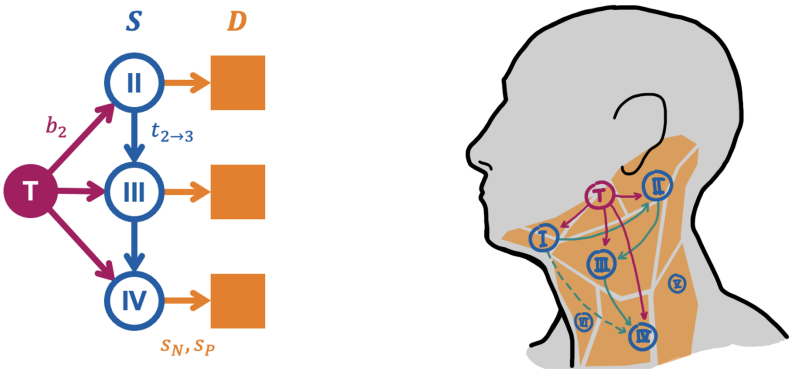

Figure 4: To graphical depictions of the idea of the lymphatic spread model reduced to only 3 LNL for simplicity [4].

The different arcs were combined in a comprehensive statistical model to predict the probability of occult metastasis in each LNL. The model is based on a Bayesian approach, more precisely a Hidden Markov model (HMM). The HMM is used to describe the spread of through the lymphatic system over time. The model parameters are sampled with Markov Chain Monte Carlo sampling. The true state of involvement and the clinically observed involvement are linked via the sensitivity and specificity. [4, 6–8]
Once the model is trained, it can be used to predict the probability of occult metastasis for each LNL for individual patients. The model takes the following inputs: clinical involvement per LNL, early (T1/T2) versus late (T3/T4) T-stage and whether the tumor has a midline extension or not. To define the elective CTV, the clinically negative LNL are ranked from highest to lowest in probabilities. LNL are added to the CTV-N until the cumulative risk for an occult metastasis of the remaining LNL is below 10%. The data collected and the risk prediction model are publicly available on `https://lyprox.org/`. [4, 6–8]
With the risk prediction model we can compute a personalized treatment for each specific diagnosis, as opposed to the guidelines which generalize a lot. The diagnosis specific treatment aims to irradiate less LNL. A volume de-escalation by reducing the elective CTV volume could result in less toxicity [9]. The assumption is that the side effects due to radiotherapy can be reduced by irradiating a smaller volume, while still controlling the tumor.
In chapter 3, we compare standard care and volume de-escalated treatment plans according to the lymphatic spread model. To evaluate the probability of observing side effects, different normal tissue complication probabilities (NTCP) are used to compare the two treatments and quantify the benefit of a reduced treatment volume.

3 Comparing standard care with volume de-escalate treatment plans

To show that the lymphatic spread model can reduce the occurrence of side effects, eight patients were retrospectively analyzed, where the delivered dose distribution has been compared with the dose distribution of the new elective target volumes. To compare the standard and volume de-escalated plans, different normal tissue complication probabilities for head and neck cancer were used.

3.1 Normal tissue complication probability

The increase of dose delivered to a patient to increase the chance of a tumor control is often limited by the response of normal tissue. To help a patient in the best possible way, a balance between tumor control and avoiding side effects is made.To assess the risk of side effects, the concept of normal tissue complication probability (NTCP) has been developed. The NTCP is a mathematical model that tries to predict the chance that certain side effect will occur. To develop a NTCP model, one needs to consider that different organs at risk play a role in the manifestation of a specific side effect and that different organs respond differently to radiotherapy. Additionally, pre-existing conditions of the patient need to be considered. A very common way to express the NTCP is a sigmoid curve: [3, 10]

$$NTCP = (1 + e^{-S})^{-1} \tag{6}$$

This NTCP formula can be used for different side effects. For each complication, different values are chosen for the function S. S is a placeholder. It can include many different parameters that have an influence on the side effect the model wants to predict. The parameters and weightings are determined by collecting patient data and fitting the formula to the observed normal tissue complications by considering a variety of factors influencing the NTCP. The larger S, the higher the NTCP value. [11]

3.1.1 Xerostomia and sticky saliva

A common side effect of radiotherapy treatment in head and neck patients is the loss or reduction of saliva production. Radiation therapy can lead to xerostomia, which is known as a dry mouth. It can affect the health of the gum and teeth. To predict moderate to severe xerostomia six months after treatment, the parameter S is defined as: [11]

$$\begin{aligned} S(\text{xerostomia}) = -5.27 + (\text{mean dose parotid glands} \cdot 0.066) + (\text{age} \cdot 0.050) \\ +(\text{baseline xerostomia score} \cdot 0.916) \end{aligned} \tag{7}$$

The term with the largest weight is the baseline xerostomia score. This term will be zero if the patient has no dry mouth before the beginning of treatment. If the patient has pre-existing symptoms of xerostomia the baseline score will be set to 1. The second influential term incorporates the dose delivered to the parotid glands. For the mean dose to the ipsilateral and contralateral side are considered. The larger the dose, the larger the complication probability. The parotid glands are the main saliva producing glands, significant damage will lead to reduced saliva production. The age is factored in due to the general inverse correlation of age and saliva production. Different NTCP curves depending on the input parameters are shown in figure 5. [11]

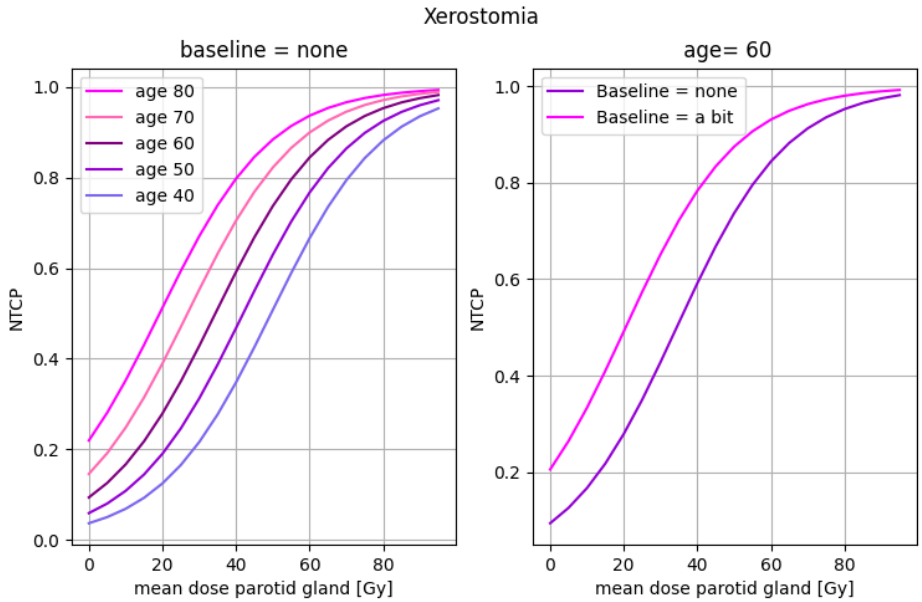

Figure 5: On the y-axis, the NTCP value for xerostomia is plotted. On the x-axis, a dose range from 0 to 100 Gy is depicted. The higher the age of the patient will increase the NTCP value. On the right side, it is shown how a pre-existing condition of dry mouth will increase the NTCP value.

Another relevant side effect in head and neck irradiation is the change of texture of the saliva, known as sticky saliva. The different consistency of the saliva can lead to trouble swallowing or stick to one's gum and teeth. A NTCP model for moderate to severe sticky saliva six months after radiotherapy is given in equation 8. [11]

$$\begin{aligned} S(\text{sticky saliva}) = 10.70 + (\text{mean dose submandibular glands} \cdot 0.091) + (\text{age} \cdot 0.107) \\ +(\text{baseline sticky saliva score} \cdot 1.218) + (\text{mean dose sublingual glands} \cdot -0.041) \end{aligned} \tag{8}$$

Two different glands that produce saliva are incorporated in this NTCP model. Interestingly, when the mean dose to the sublingual gland increases, the NTCP value decreases. The paper does not provide any insight on why this is the case. The parameter the largest weight is the baseline sticky saliva score. If the patient had symptoms of sticky saliva before treatment the baseline parameter is set to 1, else it's 0. [11]

3.1.2 Swallowing problems

After radiotherapy in the head and neck area, many patients will experience problems with swallowing food. The swallowing problems are linked to the damage due to the dose delivered to different ares of the swallowing muscles. In severe cases, patients require a feeding tube. The following NTCP model predicts the probability of a patient needing a feeding tube six months after completing treatment. [12]

$$\begin{aligned} S(\text{tube feeding}) = -11.70 + (\text{advanced T-stage} \cdot 0.043) + (\text{moderate weight loss} \cdot 0.95) \\ + (\text{severe weight loss} \cdot 1.63) + (\text{accelerated radiotherapy} \cdot 1.20) + (\text{chemo radiation} \cdot 1.91) \\ + (\text{radiotherapy plus cetuximab} \cdot 0.56) + (\text{mean dose PCM superior} \cdot 0.071) \\ + (\text{mean dose PCM inferior} \cdot 0.034) + (\text{mean dose contralateral parotid} \cdot 0.006) \\ + (\text{mean dose cricopharyngeal muscle} \cdot 0.023) \end{aligned} \tag{9}$$

All the parameters except the dose parameters are binary variables. They are either treatment or diagnosis related. Added to the binary variables are four organs at risk. The organ with the

highest weight is the pharyngeal constrictor muscle (PCM). [12]
When a patient has difficulty swallowing food, it is referred to as dysphagia. Swallowing problems are a significant toxicity during and after radiation treatment. If a patient is no longer able to eat, they will not only be weakened by the cancer treatment, but lose weight and their overall health will decline. The following models predict different problems related to dysphagia. All the models look at the side effect six months after treatment completion. [13]

- $S(\text{swallowing}) = -6.09 + (\text{mean dose PCM superior} \cdot 0.057) + (\text{mean dose supraglottic larynx} \cdot 0.037)$

As soft/solid food and liquids have different textures, the swallowing capabilities required for proper swallowing are different. Thus dysphagia is split up into problems in swallowing liquids, soft food, and solid food. [13]

- $S(\text{liquids}) = -5.98 + (\text{mean dose supraglottic larynx} \cdot 0.074) + (\text{radiation technique} \cdot -1.209)$

The NTCP for swallowing liquids heavily depends on which radiation technique is used. If IMRT is done, then the NTCP gets reduced greatly. For IMRT, the radiation technique parameter is set to 1. For three-dimensional conformal radiotherapy (3D-CRT), the radiation technique variable is set to 0. [13]

- $S(\text{soft food}) = -5.83 + (\text{mean dose middle PCM} \cdot 0.061) + (\text{age} \cdot 1.203) + (\text{tumor site} \cdot 1.122) + (\text{radiation technique} \cdot -0.912)$

For problems with soft food, the age of the patient is important. In this case, it is a binary variable that is set to 1 for patients 65 and older and set to 0 for patients below the age of 65. Another parameter is the tumor site. For patients with oropharynx and nasopharynx tumors, the parameter is set to 1. This means that patients with these two tumor sites have more problems swallowing soft food. For all other sites, the binary variable is 0. [13]

- $S(\text{solid food}) = -6.89 + (\text{mean dose superior PCM} \cdot 0.049) + (\text{mean dose supraglottic larynx} \cdot 0.048) + (\text{age} \cdot 0.795)$

For the NTCP that predicts swallowing problems for solid food, a different constellation of already described parameters is used. Head and neck cancer patients can experience choking while swallowing, due to the damage from radiotherapy. [13]

- $S(\text{choking}) = -7.07 + (\text{EIM V60} \cdot 0.020) + (\text{mean dose supraglottic larynx} \cdot 0.066)$

A new organ at risk gets added: the esophagus inlet muscle (EIM). V60 refers to the volume that receives 60% or more of the prescribed dose. [13]

3.1.3 Hypothroidism

The last NTCP looked at predicts hypothyroidism occurring in the first two years after treatment. If the thyroid is damaged, then the thyroid does not produce enough hormones. This NTCP was added, because with the new predicted treatment regime, we deliver less dose further down the neck, where the thyroid is. [14]

$$S(\text{hypothyroidism}) = 0.011 + (\text{mean dose thyroid gland} \cdot 0.062) + (\text{thyroid gland volume} \cdot -0.19) \quad (10)$$

The more dose to the thyroid gland is delivered, the higher the NTCP value will be. A bigger thyroid gland volume will reduce the NTCP. [14]
These nine NTCP models are now used to quantify the difference between the current treatment plan and the treatment plan with reduced elective volume.

3.2 Data preparation

The treatment plan was recalculated with reduced elective CTV according to the lymphatic spread model. For the comparison, only the PTV 3, consisting of the electively irradiated LNLs, was modified. The new reduced PTV 3 with all the relevant patient characteristics are listed in table 1.

#	T-stage	midline	metastases ipsi	metastases contra	guideline ipsi	guideline contra	reduced ipsi	reduced contra
1	T2	True	II	II	I-V, VII	I-V, VII	II, III	II, III
2	T2	True	none	none	II-IV, VII	II-IV, VII	II	II
3	T4	True	II, III	none	I-V, VII	II-IV	II, III, IV	II
4	T4	True	none	none	I-IV	II-IV	II, III	II
5	T3	True	I, II	III	I-V, VII	I-V, VII	I, II, III	II, III, IV
6	T3	True	none	none	I-IV, VII	II-IV, VII	II, III	II
7	T1	False	I, II	none	I-V, VII	II-IV	I, II, III	none
8	T2	False	II	none	I-V	II-IV	II,III	none

Table 1: Table of the eight replanned patients with their old and new treatment regime. First, the tumor stage is listed, which describes the size of the tumor and its duration of growth. If the tumor did grow over to the other side of the head, then the row midline is listed as true. For each patient, the detected metastases in each LNL are listed separately for the contra and ipsilateral side. The treatment given by the guideline and by the lymphatic spread model (reduced) are split in LNLs, contra and ipsilateral side. For all the patients, there is a clear reduction in the lower LNL (IV, V). For patient 7 and 8 the new treatment leaves out the contralateral side.

The new plans clearly reduce the target volume. If a level has a metastasis it is automatically included in the target volume. LNL I only gets irradiate if it is involved. In the new plans LNL V is never irradiated. LNL IV only is included if LNL III is involved. If the patient is early T-stage and has no midline extension, then the whole contralateral side can be spared. For all patients, the contralateral side is spared more than the ipsilateral side.
The calculation of the new radiotherapy plans was done in Eclipse using the clinically delivered plan as starting point. All parameters of the clinically delivered plan were kept, only the size of the elective target volume changed. For the optimization of the plans the same objectives and constraints, as in the original plane, were used. To control whether the plan was comparable to the original, the clinical goals were compared and checked whether the dose to the PTV was conformal.
To calculate the NTCP values, the relevant information for each patient was extracted from the patient data (see table 2). Most of the required information was available in the patient dossier in the hospital, except the baseline sticky saliva score for equation 8. For this equation, the NTCP with a positive baseline and a negative baseline were calculated.

#	age	baseline xerostomia	weight loss	chemoradiation	accelerated RT	cetuximab	IMRT	oropharynx	thyroid volume $[cm^3]$
1	52	True	moderate	True	False	False	True	True	14.5
2	66	True	moderate	False	False	False	True	True	8.6
3	69	False	moderate	True	False	False	True	True	34.9
4	68	False	severe	True	False	False	True	True	10.1
5	78	True	moderate	True	False	False	True	True	20.5
6	59	False	moderate	True	False	False	True	True	10.7
7	56	False	no loss	True	False	False	True	True	9.1
8	49	True	no loss	True	False	True	True	True	12.4

Table 2: All the treatment and patient related binary variables listened in a table. The treatment modalities of the patients are similar. Some of the patients already experienced side effects in the form of weight loss or xerostomia. The binary variable sticky saliva is not recorded by the hospital.

Since not all the structures needed were contoured by default, the missing ones were manually added. To contour the sublingual glands, the approach of Van de Water et al. was consulted [15]. From there we decided to take the front half of the oral cavity. The oral cavity was contoured a priori, which allowed an adaptation to build a sublingual glands structure. The hospital puts most of the swallowing muscles in the neck in one structure, the PCM. Following two papers [16, 17] the swallowing muscles were contoured with more detail. The PCM was split and extended to: supraglottic larynx, cricopharyngeal, esophageal intel muscle, PCM superior, PCM middle and PCM inferior. A rough guideline can be seen in figure 6. Once the missing structures are contoured and the plan is recalculated, the NTCPs were evaluated.

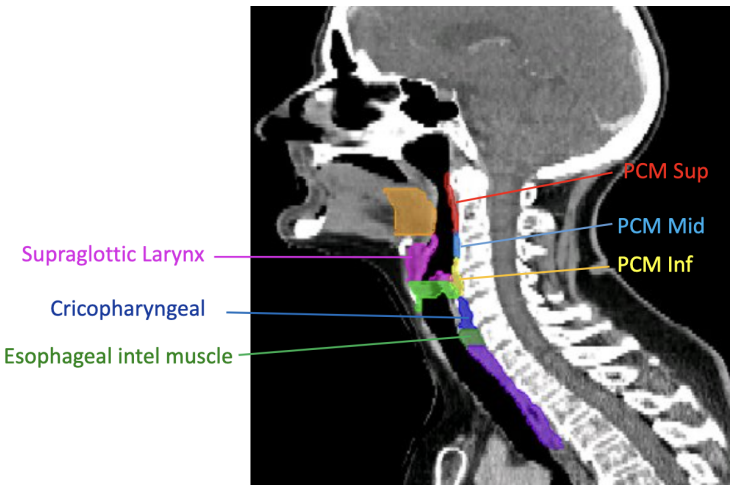

Figure 6: The six missing contours of the neck area located in a CT image [16].

3.3 NTCP calculation and plan comparison

To calculate NTCP models, the dose volume histograms (DHV) and the dose distribution in the different OAR are required. Eclipse provides the DVHs and dose distributions automatically for each contoured structure. To compare the dose reduction of the relevant organs, the dose values for the old and new plans are listed in table 3.

#	**parotid**	**submandibular**	**sublingual**	**PCM sup**	**PCM mid**	**PCM inf**	**contra parotid**	**cricopharyngeal**	**supraglottic larynx**	**V60 EIM [cm^3]**	**thyroid**
1	17.1	50.6	25.4	50.4	38.0	18.6	16.8 L	18.6	34.5	7.5	31.2
1	17.9	46.7	25.4	45.9	32.9	17.0	18.0 L	16.6	34.7	2.5	13.8
2	13.3	36.3	18.9	47.9	42.3	23.2	12.4 L	19.2	31.8	32	38.6
2	13.7	36.2	17.9	48.3	42.9	22.7	12.5 L	2.6	25.5	0	0.7
3	14.4	46.7	42.9	36.1	48.1	46.0	11.9 L	28.8	47.7	35	28.6
3	14.7	48.2	44.1	37.7	48.6	45.8	12.4 L	28.7	46.7	7.5	24.0
4	35.0	34.0	49.0	50.2	46.8	22.7	14.3 R	14.0	42.5	0	36.5
4	35.1	34.0	49.5	50.2	47.2	26.0	15.2 R	3.0	43.1	0	1.2
5	18.2	51.0	38.1	43.7	49.8	43.1	15.6 L	28.1	37.8	36	37.3
5	17.8	47.2	37.4	44.2	49.9	43.0	15.0 L	26.0	35.8	24	30.4
6	21.2	39.5	25.6	50.0	50.1	41.4	16.4 R	15.4	40.0	35	43.0
6	22.1	39.5	27.0	50.1	50.4	41.2	16.3 R	18.5	37.8	0	10.9
7	16.9	42.3	26.0	38.1	42.0	42.3	13.2 L	39.1	37.8	53	44.7
7	13.0	34.5	24.0	33.9	35.4	34.2	5.1 L	33.3	34	40	10.6
8	10.8	38.2	24.5	46.3	41.1	30.7	9.9 L	27.7	36.1	7.5	44.3
8	9.9	33.7	22.5	45.4	35.9	20.6	6.9 L	21.8	23.2	4	17.5

Table 3: Comparison of mean dose in Gray [Gy] for the old and new plans, for the relevant organs. V60 EIM is given in cm^3. The old plans are marked gray. For the contralateral parotid, it's specified whether it's the left (L) or right (R) gland.

There is a clear mean dose reduction in the organs further down the neck for nearly all patients. Which can be explained by the fact that LNL IV and V are left out of the PTV 3 in the new plan. For Patient 7 and 8 there is an overall reduction of mean dose, due to the fact that the whole contralateral side is excluded from the PTV 3. Patient 4 has the smallest overall reduction, due to the primary tumor being too large, such that it extends down to LNL III. In some cases there is no difference or even a slight increase in dose with the new plan, such as in the parotid glands of patient 1. When there is no change or only a minimal difference, it is due to the same LNLs being irradiated in both plans. Small increases or decreases in dose can occur due to the optimization process taking different paths, even when the goals remain the same. Sparing the parotid glands is rather difficult, because they are located adjacent LNL II and most of the time LNL II is irradiated. Dose reduction in the contralateral parotid gland is only possible if the

whole contralateral side is spared, such as in patients 7 and 8. The submandibular and sublingual glands get significantly less dose if LNL I is left out. But even when LNL I is not included, often the primary tumor is close or too large, such that there is only a small dose reduction. sparing the PCM is difficult, since a big part often lies in the target volume of the primary tumor. If the contralateral side can be spared, then a large dose reduction in the PCM is possible. For the remaining OARs, a reduction is nearly always achieved by not irradiating LNL III-V, which are often omitted according to the lymphatic spread model. To better estimate the clinical relevance, we calculated the NTCP values for the introduced models.

The NTCP values for the all patients are computed with the information from table 2 and 3 and the NTCP models introduced in chapter 3.1. The results of the different NTCP values are listed in table 4.

#	**xerostomia**	**sticky saliva [0]**	**sticky saliva [1]**	**tube feeding**	**swallowing**	**liquids**	**soft food**	**solid food**	**choking**	**hypothyroidism**
1	34.9%	17.2%	41.2 %	4.2%	12.6%	1%	3.6%	5.9%	1%	30.8%
1	36.1%	12.7%	33.0%	3.0%	10.1%	1%	2.5%	4.9%	0.9%	13.1%
2	66.1%	24.8%	52.7%	0.6%	10.1%	0.8%	13.7%	9.8%	1.3%	68.4%
2	66.5%	25.4%	53.5%	0.4%	8.4%	0.5%	14.2%	7.6%	0.5%	17.1%
3	29.5%	30.4%	59.7%	5.5%	9.4%	2.5%	18.5%	11.5%	3.8%	0.8%
3	29.0%	32.3%	61.8%	6.2%	9.9%	2.3%	19.0%	11.9%	2.1%	0.6%
4	60.8%	8.8%	24.6%	11.6%	16.0%	1.7%	17.3%	16.9%	1.4%	58.8%
4	61.0%	8.6%	24.2%	12.3%	16.3%	1.8%	17.7%	17.3%	1.4%	13.6%
5	67.9%	67.4%	87.5%	9.0%	10.0%	1.2%	20.1%	10.5%	2.1%	17.2%
5	67.3%	60.1%	83.6%	9.0%	9.6%	1.1%	20.2%	9.9%	1.4%	11.9%
6	28.5%	13.7%	34.9%	12.1%	14.7%	1.4%	7.1%	7.4%	2.3%	65.6%
6	29.7%	13.0%	33.6%	12.3%	13.8%	1.2%	7.3%	6.8%	1.0%	20.6%
7	20.5%	12.7%	33.0%	1.5%	7.4%	1.2%	4.5%	3.9%	2.9%	74.1%
7	16.6%	7.2%	20.8%	0.7%	5.2%	0.9%	3.0%	2.7%	1.3%	25.7%
8	23.4%	4.8%	14.7%	2.4%	10.3%	1.0%	4.2%	5.0%	5.4%	59.9%
8	22.4%	3.5%	11.0%	1.7%	6.6%	0.4%	3.1%	2.8%	0.4%	22.1%

Table 4: The probabilities that the different NTCP models predict. The values for the old plans are marked in gray. Since the baseline for sticky saliva is not known, both NTCP values are calculated with the baseline equal to 0 and 1.

The best results are achieved if the contralateral side is not included into the elective target volume. For patient 7 and 8 each NTCP value is reduced with the new treatment plan. These are early T-stage patients, that means, the tumor had less time to spread, therefore, the model proposes to irradiate a smaller elective volume.
In most of the cases, there is no significant difference. Either because the predictions had low value initially, as in the case of the NTCPs for swallowing liquids or choking. Or because the

different NTCP models do not weight the dose parameters as strongly as the binary variables, which do not change between the two plans. The largest reduction is possible for the prediction of getting hypothyroidism. In the de-escalated plans we irradiate less volume in the caudal neck areas, which will lead to less dose to the thyroid.
Not all the NTCP models are as good at capturing this change. This can be due to there weighting of the binary variables that are stronger than there dose dependent counterparts. Another factor is that in some of the relevant organs we see no change in the mean dose value. Still overall there are less side effects due to reduced volume.

4 Tumor control probability

In the second part of the thesis, we want to develop a tumor control probability (TCP) model which includes the probability of occult metastases obtained from the lymphatic spread model. The TCP model is then applied in treatment plan optimization. These treatment plans which are based on TCP and NTCP should better balance the trade-offs. In a first step, TCP models in general are discussed before the probabilistic TCP model is introduced.

With the tremendous technological advancement in radiotherapy, treatment planning and treatment delivery have become more complex. The assessment of the quality of a treatment plan, became more difficult. Traditionally, radiotherapy outcomes have been modelled with the information given by the dose distribution and the fractionation pattern. This information does not paint the full picture. The radiotherapy outcomes are often affected by multiple clinical and biological factors. In general, the tumor response will increase with higher dose, but there are other factors to consider. A simple way to evaluate multiple factors combined is to consider the tumor control probability. [1]
The TCP is defined by the probability of the extinction of clonogenic tumor cells at the end of treatment. The tumor control probability attempts to measure how likely it is to control the tumor [10]. A TCP model has a sigmoid shape, similar to the shape of a NTCP model. There are different ways to mathematically describe such a curve including the Poisson, the logistic and the probit models. These models are fitted to clinical or experimental data to obtain a predictive TCP model. All three models often lead to very similar results. We take a closer look at the logistic models, since these models are later used to calculate the probabilistic TCP values in this work. [1]
The logistic model is a flexible model to estimate tumor response probabilities. The idea of the logistic model is to write the probability of an event (P) as:

$$TCP = P = \frac{e^u}{1 + e^u} \tag{11}$$

The function u can incorporate different treatment characteristics or patient related information. An important factor included is the dose to the tumor. In the logistic model, TD_{50}, representing the radiation dose for 50% tumor control, and m_{50}, indicating the curve's steepness at TD_{50}, are utilized as model parameters. [1]
Clinical and experimental evidence support the model, since data indicates that the TCP increases with increasing dose. Sufficient radiation dose will therefore control nearly any tumor. However, arbitrarily high doses are often not possible due to surrounding OAR. Often a trade-off between TCP and NTCP needs to be found, as depicted in figure 7. [18, 19]

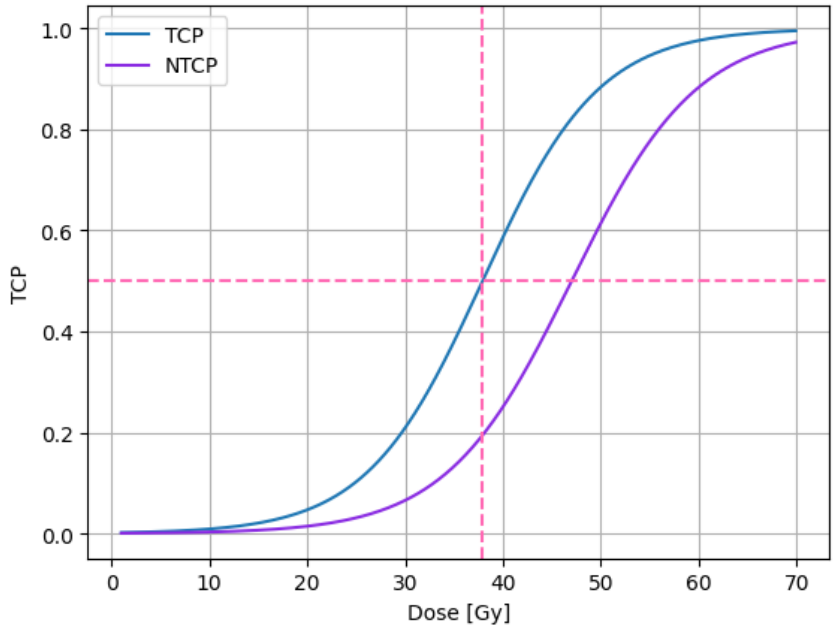

Figure 7: Plot of TCP (blue) and NTCP (violet) in one figure. The pink dashed line marks the TD_{50} value in the TCP model. The larger the dose delivered to the tumor, the higher the TCP. But with increasing dose, the chance of a side effect increases as well.

Since the TCP represents a probability it can take values from 0 to 1. In absence of a tumor, the TCP will be 1 no matter how much dose is delivered. The higher the TCP of a treatment plan, the better the plan in regard to controlling the tumor. [1]
For our TCP model, we will build upon the TCP model introduced by Okunieff et al. (1995) [18] as the foundation.

$$TCP_{ok} = \frac{e^{\frac{d-TD_{50}}{\frac{25}{m_{50}}}}}{1 + e^{\frac{d-TD_{50}}{\frac{25}{m_{50}}}}} \tag{12}$$

The model depends on the dose (d) delivered, the TD_{50} and m_{50} value, that are estimated in the paper. The model is plotted in figure 7 with the TD_{50} value marked by the crossing of the dashed pink lines. The TD_{50} values are computed from the dose of radiation that locally controls 50% of the tumors in human subjects with a logit analysis and a least squares algorithm. The m_{50} values were computed with a logit function and the TD_{50} values. To do this, data from different institutions was collected. For microscopic disease, the paper gives the following TD_{50} and m_{50} values. [18]

$$TD_{50ok} = 37.9 \quad m_{50ok} = 4.2 \tag{13}$$

The presented TCP model is validated for entire microscopic tumors with a homogeneous dose distribution. However, in our application, we want to divide the volumes at risk of harboring microscopic metastases into subregions. From there, we want to be able to deliver inhomogeneous dose distributions to the target. Therefore, the TCP model by Okunieff et al. needs to be generalized from homogenous to inhomogeneous dose distributions.
To create a model that can handle inhomogeneous dose distributions, we need to know how likely it is that each LNL is involved. In chapter 2.4 we introduced a model that predicts probabilities for each LNL being involved based on a given diagnosis. An example of such a prediction is shown in figure 8.

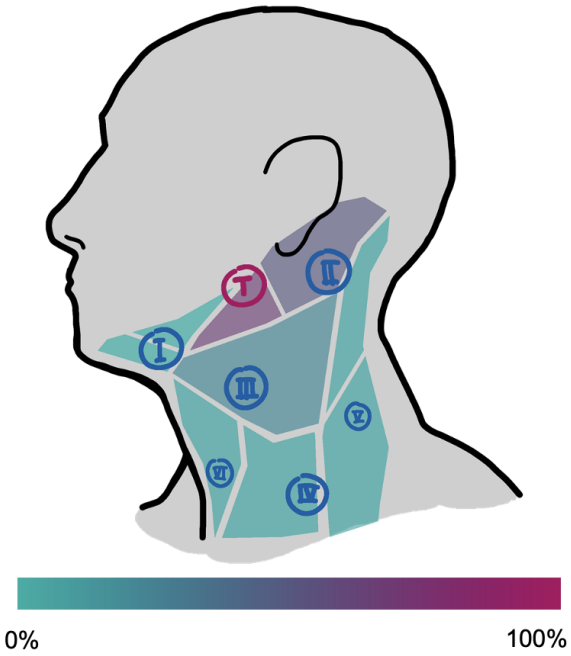

Figure 8: Example of probability distribution in the different LNL where LNL II has a high probability of being involved.

The probability that this model produces, we will call Q the overall probability of microscopic involvement in a LNL. With, Q we can generalize TCP_{ok} as:

$$TCP_Q = \underbrace{Q * TCP_{ok}}_{\text{involved}} + \underbrace{1 - Q}_{\text{healty}} \tag{14}$$

TCP_Q can be split up into an involved and a healthy part. If the volume is not involved, then Q will be 0 and TCP will be equal to 1 even though no dose is applied. With this adaptation, we will later be able to build our probabilistic model on the generalized Okunieff model (TCP_Q).

4.1 Probabilistic clinical target volume concept

The paper from Bortfeld et al. (2021) [20] introduces the idea of a probabilistic clinical target volume and its consequences for the optimization of the TCP in treatment planning. The clinical standard is to consider a binary CTV where the cells or tissue around the tumor are either involved or not. A probabilistic CTV assigns each subvolume around the tumor a probability of containing microscopic tumor tissue. The new CTV consists of many subvolumes. Each subvolume has a probability of being involved. The paper provides a method to optimize a treatment plan based on the probabilistic CTV. While the idea for a probabilistic CTV has been around for a while, commercial treatment planning systems are not compatible with probabilistic CTVs yet. One of the main obstacles has been the assignment of probabilities of microscopic involvement to different volumes, which was not realistically feasible in most cases. With the lymphatic spread model however, we can compute probabilities to different volumes and investigate realistic applications of the concept. [20]
Bortfeld et al. introduce two different TCP models which implement the probability of microscopic involvement in each subvolme differently.

- One model assumes that the subvolumes are independent of each other. Each subvolume has a probability of having a microscopic tumor spread independent of the involvement state of the surrounding subvolumes. [20]

- The second model assumes that the subvolumes are not independent. The subvolumes further away from the GTV can only be involved if all the subvolumes between it and the GTV are involved. There has to be a path that connects them. [20]

The second approach is closer to the real behavior of tumor cells in the case of the primary tumor CTV. Here we will use the idea of the independent subvolumes in part for simplicity, but also because we consider the nodal CTV, where tumor cell have no connection to the original tumor and often stand alone. Bortfeld et al. introduced an overall TCP that is the product of all subvolume TCPs and their probability of being involved: [20]

$$TCP = \prod_{i=1}^{N}(1 - q_i + q_i * TCP_i) \tag{15}$$

Where N is the number of subvolumes, q_i is the probability of subvolume i being involved and TCP_i is the TCP of the subvolume i, depending on the dose it receives [20].
Bortfeld et al. applied the TCP model on a theoretical phantom with heuristically chosen involvement probabilities. The goal of this thesis is to construct a treatment plan for a real oropharyngeal cancer patient based on a TCP optimization which considers the probability of involvement of different lymph node. At the time of writing, no model that can handle a subvolume TCP on a voxel level was available.

4.2 Probabilistic TCP

To setup the TCP from equation 15 we first need to define what the extent of a subvolume is and their respective probabilities of involvement q_i are. Further, the TCP model used and the different values to define the TCP model need to be specified.
The overall probability of microscopic involvement in a level is given as Q, which can be calculated by the lymphatic spread model. We now assume that in the whole LNL, the probability of occult metastasis is uniform. In addition, we assume that all subvolumes have the same size. With these two assumptions, each subvolume will have the same probability of being involved. The probability that the LNL is healthy is:

$$(1 - Q) = (1 - q)^N \tag{16}$$

N is the number of subvolumes and q is the probability of a subvolume. This equation can be rearranged to:

$$q = 1 - \sqrt[N]{1 - Q} \tag{17}$$

This means the TCP from equation 15 simplifies to:

$$TCP_q = \prod_{i=1}^{N}(1 - q + q * TCP_i) \tag{18}$$

TCP_q is the probability of the whole volume. This is the value that we later want to maximize in our optimization. TCP_q depends on all the voxels in the volume (N) and on the probability of controlling each voxel. For TCP_i we will take the model previously introduced from Okunieff (eq. 12). The TD_{50} and m_{50} can not simply be copied, because they were calculated for a homogeneous dose distribution, but we want a model that considers each voxel and can handle an inhomogeneous dose distribution. We chose the two missing parameters such that we get the same result for a homogeneous dose distribution as the modified Okunieff model from equation 14. We can rewrite equation 18 as:

$$P(1+) * TCP_q + P(2+) * TCP_q^2 + ... + P(N+) * TCP_q^N \tag{19}$$

$P(1+)$ is the probability of exactly one subvolume involved. If the voxel is involved the TCP can have a value between 0 and 1. If k volumes are involved ($P(k+)$) then for each volume the TCP has to be calculated separately. The probability of exactly k voxels involved is given as:

$$P(k+) = q^k(1-q)^{N-k}\binom{N}{k} \tag{20}$$

To now find the missing two values we can consider that Q can be split up into a binomial distribution.

$$Q = \sum_{k=1}^{N} q^k(1-q)^{N-k}\binom{N}{k} \tag{21}$$

Q is equal to the sum of all the possible combinations of voxels involved. From this we know that the involved part of the equation 14 contains all the possible combinations where one or multiple subvolumes are involved. To now find the missing TD_{50q} and m_{50q} we evaluate the expression:

$$Q * TCP_{ok} \approx P(1+) * TCP_q + P(2+) * TCP_q^2 + ... + P(N+) * TCP_q^N \tag{22}$$

Equation 22 can now be used to find the TD_{50q} and m_{50q} values for the TCP_q model. For the left side of equation 22 we plug in the known TD_{50ok} and m_{50ok} values. The TD_{50q} and m_{50q} values for the TCP_q model are then calculated through a least squares fit approach.

4.2.1 Least square fit

A least squares fit (LSQ) is a type of regression analysis used to determine the curve for a set of data points. This method minimizes the sum of the squared differences between the observed data points and the values predicted by the model. By calculating the squared distances between each observed data point and the corresponding predicted point, and then summing these squared distances, we obtain a measure of the goodness of fit. The values with the smallest sum of squared distances is considered the best fit. [21]

$$LSQ = \min_x \sum_{i=1}^{n} (y_i - M(x_i))^2 \tag{23}$$

The given data points y_i are in our case the values generated by the left side of equation 22.

$$Q * TCP_{ok}(TD_{50}, m_{50}, d_i) = Q * \frac{e^{\frac{d_i - TD_{50}}{\frac{25}{m_{50}}}}}{1 + e^{\frac{d_i - TD_{50}}{\frac{25}{m_{50}}}}} \tag{24}$$

We looked at a dose range from 0 to 70 Gy, with a spacing of 0.1 such that we generated 700 data points that we can compare to. We now need to fit the right side of equation 22 to the generated data points.[21]

$$M((TD_{50q}, m_{50q}), d_i) = P(1+) * TCP + ... = q^1(1-q)^{N-1}\binom{N}{1} * \frac{e^{\frac{d_i - TD_{50q}}{\frac{25}{m_{50q}}}}}{1 + e^{\frac{d_i - TD_{50q}}{\frac{25}{m_{50q}}}}} + ... \tag{25}$$

To find the best TD_{50q} and m_{50q} values two, arrays with possible values were generated. After the first run we saw that the values are very similar to the literature values. The range of values was narrowed down to find the best possible fit. [21]
Evaluating equation 25 is demanding. The more subvolume one chooses the more entries the right side of equation 22 gets. Since we want to consider each voxel in the target we want to estimate the TD_{50q} and m_{50q} values for more than 1000 subvolumes.

To reduce the computation time one can prove that it is enough to only look at a subset of entries encompassing the first terms in the sum, because the rest of the sum gets small enough to be neglected.

Proof:
We want to prove that for sufficiently large n $(1 < n < N)$ the sum of the additional terms are below a threshold ϵ and be discarded.

$$I.e. \sum_{i=n}^{N} q^i (1-q)^{N-i} \binom{N}{i} << \epsilon \tag{26}$$

Use:

$$\binom{n}{i} \leq \left(\frac{e*n}{i}\right)^i \tag{27}$$

Proof: $\binom{n}{i} \leq \left(\frac{e \cdot n}{i}\right)^i$ [22]:

$$\binom{n}{i} = \frac{\prod_{j=0}^{i-1}(n-j)}{i!} \leq \frac{n^i}{i} \leq \left(\frac{n*e}{i}\right)^i \tag{28}$$

This can be used to show that the sum can be cut.

$$\sum_{i=n}^{N} q^i (1-q)^{N-i} \binom{N}{i} \leq \sum_{i=n}^{N} q^i (1-q)^{N-i} \left(\frac{N*e}{i}\right)^i \tag{29}$$

$$= \sum_{i=n}^{N} \underbrace{(1-q)^{N-i}}_{<1} \left(\frac{N*e*q}{i}\right)^i \tag{30}$$

$$\leq \sum_{i=n}^{N} \left(\frac{N*e*q}{i}\right)^n \tag{31}$$

$$\tag{32}$$

if

$$\frac{e*N*q}{n} < 1 \tag{33}$$

then

$$\sum_{i=n}^{N} \left(\frac{N*e*q}{i}\right)^n < (N-n) \left(\frac{N*e*q}{n}\right)^n \tag{34}$$

$$\Rightarrow \sum_{i=n}^{N} q^i (1-q)^{N-i} \binom{N}{i} < (N-n) \left(\frac{N*e*q}{n}\right)^n \tag{35}$$

n is the place where one would cut off the rest of the sum. For example $N = 1000$, $n = 100$, $Q = 0.08$ which gives $q = 0.0008$ this leads to:

$$\sum_{i=n}^{N} q^i (1-q)^{N-i} \binom{N}{i} < (N-n) \left(\frac{N*e*q}{n}\right)^n = 900 * \left(\frac{1000*e*0.0008}{100}\right)^{100} = 4.9 * 10^{-164} \tag{36}$$

This shows that the entries in equation 19 from a 100 upwards only sum up to a very small number that can be neglected. Thus, a large part of the sum to calculate in equation 22 can be cut off with no real impact on the result, improving the computation time drastically.
From this, it is clear that for a 1000 subvolumes (N) and an overall probability (Q) of 0.08 only

the first 100 entries of equation 22 need to be calculated. The resulting values from the least square fit were:

$$\mathbf{TD_{50q} = 37.65 \quad m_{50q} = 4.2} \tag{37}$$

These two values are very similar to the original values. This indicates that the new TCP model is primarily influenced by the scenario where one voxel is involved. The two values were calculated for $Q = 0.08$ and $N = 1000$. For different values of Q and N, the TD_{50} and m_{50} values will change slightly because the calculation depends on these parameters. The changes were minimal for realistic inputs, so we decided to use the values from equation 37.

4.3 Validation of TCP_q

To validate our new TCP model, we will look at dose distributions and their corresponding dose volume histogram DVH. Then we calculate the corresponding TCP_q values to see whether they yield the desiered result.
For example, if the whole target receives 50 Gy the TCP value should be higher than 99%. This can be deduced from the TD_{50q} and m_{50q} values taken from the model. 50 Gy on the whole volume should kill nearly all tumor cells and with that reach a high TCP value. What we are especially interested in is to see how the TCP model behaves for a non-uniform dose distribution in the targeted level. If only 50% of the level receives the 50 Gy, then only the voxels receiving the prescribed dose should be controlled. If the probability of occult disease Q is 8% then the TCP value should at least be 92% to start with. The resulting TCP should be around 96%, since 50% of the voxels are controlled, adding another 4% to the TCP. For the cases of complete, half and no irradiation of one LNL, the DVH is plotted in figure 9.

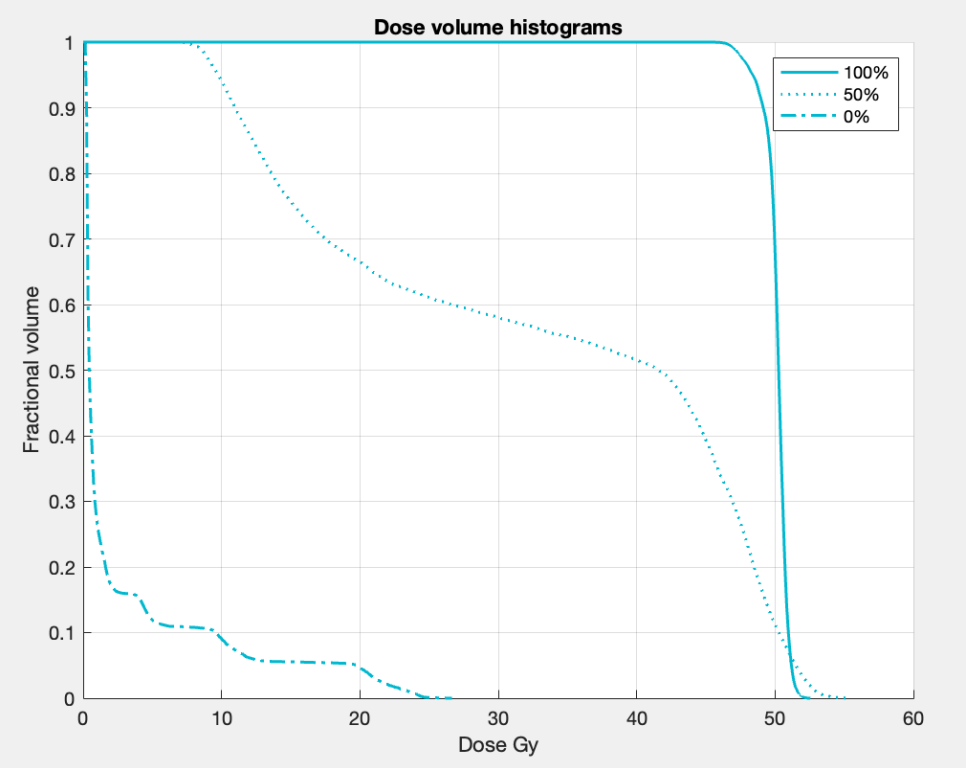

Figure 9: DVH curves for the cases that: 100% of the volume receives the prescribed dose, only 50% of the target receives the prescribe dose and no dose is delivered to the level.

The DVH show how much of the target volume receives the prescribed dose of 50 Gy. For the case where the whole level is irradiated, the DVH shows that nearly the whole volume receives

50 Gy. For the second case, 50% of the subvolumes receive around 42 Gy. The desired 50 Gy is not reached, probably due to us trying to spare the other half completely. The last case is not fully reached due to the dose constraints of the other PTVs. Still very little dose is delivered. For each of these DVHs the TCP_q was calculated.

$$\begin{aligned} 100\%: &\rightarrow \ TCP_q = 99.1\% \\ 50\%: &\rightarrow \ TCP_q = 95.6\% \\ 0\%: &\rightarrow \ TCP_q = 92.1\% \end{aligned}$$

The TCP_q values are very similar to what we expected from the model and seam reasonable. Now that we have a validated TCP model, we can proceed with the optimization of our treatment plan.

5 Implementation of a treatment plan optimization

During this thesis, new treatment plans were calculated for 4 patients. The process of the planning and optimization is show for one example patient.
The planning and optimization work was done in Matlab. First, the patient data was anonymized and extracted from the clinics' treatment planning tool Eclipse as DICOM files and then transferred to Matlab. The exports include the patient's CT pictures and the contoured structures. To handle the DICOM files in Matlab additional software is required.

5.1 A computational environment for radiotherapy research

The software we used is called the computational environment for radiotherapy research (CERR). It is a software for treatment planning research [23]. CERR can be installed into Matlab. From there, we can convert the exported DICOM files into a Matlab file, such that they can be viewed and handled in Matlab. In CERR, we have the capability to contour missing structures or modify existing ones. Additionally, CERR can generate dose deposition matrices for each beam angle and beamlets specifically for the target structure. The beamlets have the size 0.5x0.5 cm^2. For our case, we have chosen 15 beam angles for good target coverage. The target is the primary target volume combined with the elective target volume. The sampling rate was set to 2. In CERR, a sampling rate of 2 means that for every two units or intervals, a dose value is recorded, simplifying the data collection process. With the function *write_ konrad_ dij_ from_ cerr* the D_{ij} matrix can be extracted and saved from CERR for later use.
The software can generate a structure file that holds all the structural information of the patient. The function *make_ vv_ and_ voi_ from_ cerr* will generate a voi file that is later used. The problem with the voi file is that a voxel can not belong to two structures. To solve that problem, the script *mask_ generator* is run, to generate a mask for each structure bypassing the problem. The voi file is still needed for other additional information.
Additionally, we used CERR to look at dose distributions with the function *ju_ load_ downsampled _ dose* and we made use of the falloff dose generative function *find_ geometric_ fall_ off_ dose*. CERR can also generate dose volume histograms from loaded dose distributions.
From CERR we can generate all the material we need to create our own treatment plan optimization in Matlab.

5.2 Interior point optimizer

We decided to use the interior point optimizer (Ipopt) software package. Ipopt is designed to find solutions for mathematical optimization problems shown in equation 2. The constraints and objectives can be nonlinear and nonconvex [24].
The optimization framework used in a previous paper ([25]) served as the starting point and was adapted and adjusted to suit the requirements of the current problem.

5.3 Quadratic objective

To enable Ipopt to function, the only missing components are the objective it should minimize and the gradients required for optimization. In our scenario, we employed four objectives. These four objective are in the following, demonstrated at patient 6 from table 1. We can take a look at the risk prediction for the different levels to determine the elective CTV (table 5). The risk predictor is online on `https://lyprox.org/riskpredictor/4/`. To predict a specificity of 100% and a sensitivity of 81% were used. The elective target volume as defined as LNL II, III ipsilateral and LNL II contralateral.

#	**T-stage**	**midline**	**metastases**	**ipsi**	**contra**
6	T3	True	none	II (27%), III (4%)	II (6%)

Table 5: All the parameters that determine the risk prediction for patient 6. The LNL with a notable probability are listed.

In a first step, we want to ensure that the prescribed dose is delivered to the PTV. The prescribed dose is different for each PTV:

PTV 1: 70 Gy
PTV 2: 60 Gy
PTV 3: 50 Gy

PTV 1 is a 10 mm expansion of the GTV, PTV 2 is a 15 mm expansion of the GTV and PTV 3 is an 5 mm expansion of the elective CTV.
To deliver the prescribed dose to the PTVs, we use quadratic objectives. A quadratic objective penalizes too high or too low dose. The objective increases if the differences between the dose in the voxel and the prescribed dose gets larger. The objective takes the square of the difference, such that it is always positive. [2]

$$f_q(d) = \frac{1}{N_q}\sum_{i=1}^{N_q}(d_i - d^{max})^2 \tag{38}$$

The quadratic objective $f_q(d)$ is given by the number of voxels (N_q) in the structure, the dose in each voxel (d_i) and the prescribed maximum dose (d^{max}). The quadratic objective function can be expanded to a picewise quadratic penalty function. [2]

$$f_q(d) = \frac{1}{N_q}\sum_{i=1}^{N_q}(d_i - d^{max})_+^2 \tag{39}$$

Now with the added + the quadratic function is set to zero if:

$$d_i < d^{max} \tag{40}$$

This function only penalizes if the voxel is overdosed. We can also add a sum to penalize underdosing. We can now combine any number of objective with lower (d^{min}) or upper (d^{max}) bounds. Additionally, the different objectives can be weighted differently for upper and lower bound(w_u or w_l). So one can say that achieving the minimal dose in the whole structure is more important than overdosing in the organ. [2]

$$f_q(d) = \frac{1}{N_q}\left[w_u * \sum_{i=1}^{N_q}(d_i - d^{max})_+^2 + w_l * \sum_{i=1}^{N_q}(d^{min} - d_i)_+^2\right] \tag{41}$$

In the case of the lower bound objective the entry will be zero if: [2]

$$d^{min} < d_i \tag{42}$$

For each of the PTVs a d^{min} and d^{max} was set with different weightings listed in table 6.

Structure	$\mathbf{d^{min}}$	$\mathbf{d^{max}}$	$\mathbf{w_l}$	$\mathbf{w_u}$
PTV1	70	70	15	10
PTV2	60	60	10	1
PTV3	50	50	10	1

Table 6: To achieve the prescribe dose, the maximum and minimum dose were set to said value. Underdosing is severe than overdosing. This is why the lower weights are higher.

To find optimal values, different sets were tried and the best were taken. For each of these three structures, we get an objective that is added to the sum of objectives that is to be minimized. Now to optimize the sum of objectives, we need to compute the negative gradient. The gradient can easily be derived from equation 41.

$$\frac{\partial f_q(d)}{\partial x_j} = \frac{1}{N_q} * 2 * D_{ij} \left(w_u * \sum_{i=1}^{N_q} (d_i - d^{max})_+ + w_l * \sum_{i=1}^{N_q} (d^{min} - d_i)_+ \right) \tag{43}$$

Where the D_{ij} matrix is calculated with equation 1.
We now have set up the objective that delivers the dose to the target volume. In further steps, we want to reduce the dose to the organs at risk. First we add the fall off objective to ensure a steep dose falloff outside the target.

5.4 Falloff objective

To reduce the dose to the normal tissue, we need a conformal dose distribution. This means that there is a sharp falloff in dose moving away from the PTV. CERR has an integrated function, *find_geometric_fall_off_dose*, to generate a sharp falloff. For each of the three different PTVs a falloff condition was generated to achieve good falloff. Generally, a good falloff is defined as a 50% reduction of dose in 1cm. After the 1cm falloff, where the dose no longer changes, certain values were manually adjusted. Specifically, within the 70 Gy falloff from PTV 1, 35 Gy remained outside the PTV 1 structure. These 35 Gy were modified to 25 Gy to align with the end of the falloff from PTV 3, resulting in a falloff from 50 Gy to 25 Gy. The same adjustment was made for the falloff from PTV 2.
This falloff file was then formed to a pairwise quadratic objective with a weighting w_f:

$$f_f(d) = w_f * \sum_{i=1}^{N_b} (d_i - d_{falloff})_+^2 \tag{44}$$

This objective only applies to the voxel outside the PTVs that are part of the body N_b. Now if the dose outside the PTV is smaller than the falloff dose in said voxel, then the objective will be zero. If the dose is bigger than the falloff dose, it will be penalized. The weight was set to 0.00005. Higher weights lead to a non uniform dose distribution in PTV 3. The gradient for the falloff objective is given by:

$$\frac{\partial f_f(d)}{\partial x_j} = 2 * D_{ij} * w_f * \sum_{i=1}^{N_b} (d_i - d_{falloff})_+ \tag{45}$$

In figure 10 the different dose distributions with and without falloff objective displayed with different weighting. There is a clear difference between a dose distribution with and without falloff objective. Weighting the falloff objective too much leads to insufficient coverage of the target volume with the prescribed dose (see figure 10c).

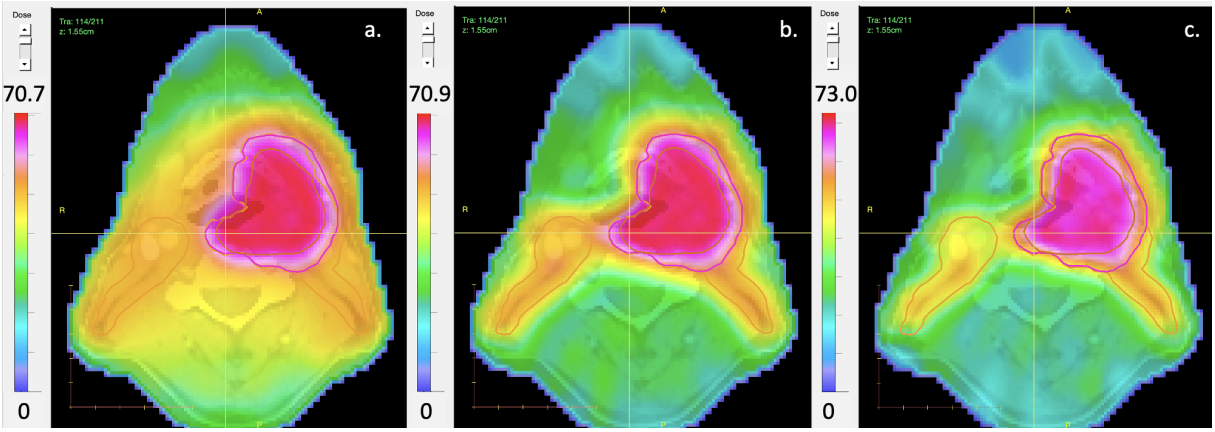

Figure 10: a.) CT image of patient 6 with a dose distribution generated only with quadratic dose objectives. PTV 1 is outlined with a pink contour, the red contour marks PTV 2 and the orange contour is PTV 3. b.) Dose distribution generated with quadratic objectives and dose falloff objective with a weight of 0.00005. c.) Falloff objective with a weight of 0.1.

In the first picture we can see a good dose conformity but a lot of dose outside the target. With the added falloff objective in distribution two we still achieve a good dose coverage but less dose outside the target. If we increase the falloff weight like in figure 10c, then no longer enough dose is delivered to the target.

5.5 Mean dose objective

To spare specific organs we added mean objectives. The mean dose objective aims to minimize the mean dose that is given to the targeted structure. For that, the sum of the dose from each voxel is taken and divided by the number of voxels in the structure to get the mean dose for the chosen structure. [2]

$$f_m(d) = \frac{1}{N_m} * w_m * \sum_{i=1}^{N_m} d_i \tag{46}$$

$f_m(d)$ is the mean objective. N_m is the number of voxels in the structure where we want to minimize the mean dose and d_i is the dose in each voxel of the structure. [2]
The gradient is given by:

$$\frac{\partial f_m(d)}{\partial x_j} = \frac{1}{N_m} * w_m * D_{ij} \tag{47}$$

We now need to decide which structure should be spared. We can take a closer look at patient 6 with his risk prediction from table 5. In this case, LNL III is the one with the lowest probability. The dose delivered to this level will later be determined with the TCP objective. Later on we want to achieve a trade-off between said LNL a mean objective. The organ that is spared should lie near the targeted level. Additionally, it should be connected to a side effect we want to avoid. In the case of patient 6 we picked the PCM.
From table 3 we see that sparing the lower part of the PCM is possible, with our reduced irradiation scheme. We now would like to spare the PCM even further. Sparing the PCM as a whole is not possible. The upper part of the muscle nearly always lies in the target volume. If we try to reduce the mean dose in the whole PCM, this will then lead to a hole in the PTV. A treatment plan with a hole in the target volume is not acceptable. To evade this problem, we split the PCM into a part the lies in the PTV and a part that is outside the PTV. Only the volume outside the PTV is used for the mean objective.
In chapter 3 we took a look at many different NTCP models for head and neck cancer patients,

In those models the PCM was split into superior, middle and inferior. We decided that to look at the PCM as a whole. Additionally, none of the models looked at all three parts of the PCM at the same time and the NTCP values are already low (see table 4). Due to these reasons, we decided to add another NTCP model.

5.5.1 NTCP for pharyngeal constrictor muscle

We need a NTCP that strongly dependeds on the PCM. Of all evaluated NTCP models, the NTCP models that predict dysphagia were best fitting. Instead of predicting late dysphagia like in equation 3.1.2 that occurs 90 days or later after completion of the treatment, the new model predicts acute dysphagia that occurs 90 days or earlier after treatment. The model has the mean dose to the whole PCM as input. The NTCP value is calculated with a logistic function of the form: [26, 27]

$$NTCP = \frac{1}{1 + (\frac{MD_{50}}{D})^k} \tag{48}$$

The parameter D is the mean dose to the PCM. The MD_{50} value is the mean dose at which 50% of the patients experience toxicity, in this case dysphagia. k describes the increase in incidence with increasing dose. The two missing values are given by: [26, 27]

$$MD_{50} = 44.5 \quad k = 2.6 \tag{49}$$

This new model is used to quantify the improvement in toxicity when trying to spare the pharyngeal constrictor muscle [26, 27].

5.5.2 Implementation mean dose objective

After discussing the mean dose objective and identifying an organ at risk, we tackled the issue of not having an appropriate NTCP model to illustrate the change in toxicity. In a first step, we are looking for a weight that spares the OAR but does not interfere with the dose coverage of the LNL. To find a good weight, we first looked at the dose distribution with no mean objective. We then compared the dose distribution without a mean objective to one with a mean objective but without weight ($w_m = 1$). The difference in the dose distribution is shown in figure 11. There is a clear difference between the two dose distributions. While both have good dose coverage of the LNL, the mean objective spares the PCM, but does not interfere with the dose delivered to the LNL without inferring with the dose uniformity in the LNL. For now, the parameter $w_m = 1$ seems like a good fit.

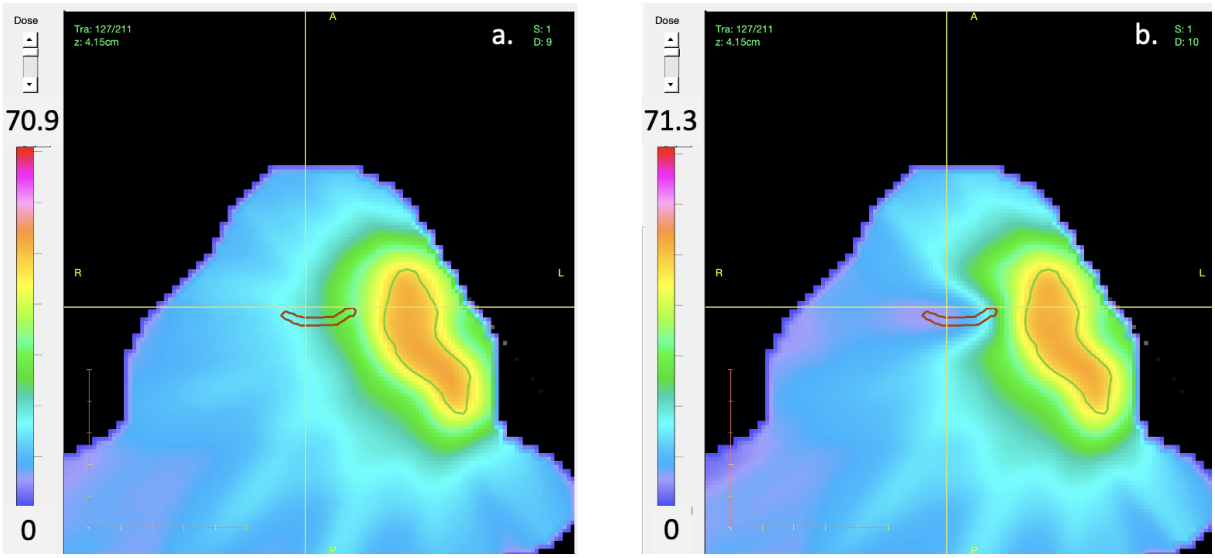

Figure 11: a.) Dose distribution with no mean objective on the PCM. The organ at risk is contoured in red, while LNL 3 is drawn in green. b.) Dose distribution with a mean objective on the PCM. The weight of the objective is set to 1 ($w_m = 1$). With this weight, there is a clear sparing of the PCM, but the LNL still received the prescribed 50 Gy for the whole area.

To compare the toxicity between the two treatment plans, we calculated the NTCP (eq. 48) for both plans.

$$w_m = 0 \quad NTCP = 63.9\% \tag{50}$$
$$w_m = 1 \quad NTCP = 59.2\% \tag{51}$$

The NTCP value is calculated on the mean dose in the whole PCM and not just the part that is outside the PTV. By adding a mean objective, the NTCP value can be reduced nearly 5%. An even bigger reduction is difficult, because in the upper section of the PCM we can not change the dose that is delivered, due to the PTV covering the PCM.
In the last step, we now add the TCP objective, based on the TCP model in chapter 4.2.

5.6 Tumor control probability objective

The last objective added is the TCP objective. With this objective, we try to optimize the treatment plan based on the TCP value. For patient 6 the target that is considered is LNL III on the ipsilateral side of the patient, thus being excluded from the quadratic objective. The dose delivered to this level is optimized based on the TCP objective ($f_{TCP}(d)$).

$$f_{TCP}(d) = w_{TCP} * \left(1 - \prod_{i=1}^{N_t} 1 - q + q * \frac{e^{\frac{d_i - TD50}{\frac{25}{m_{50}}}}}{1 + e^{\frac{d_i - TD50}{\frac{25}{m_{50}}}}} \right) \tag{52}$$

The objective calculates the TCP value for the number of subvolumes N_t. In our case, each voxel in LNL III is considered a subvolume. N_t is the number of voxels in the targeted LNL. The multiplication with -1 of the expression from chapter 4.2 is essential for incorporating the objective; whereas all other objectives are to be minimized, the TCP objective must be maximized. By multiplying with -1 we minimize the probability of tumor relapse. With the overall probability of the LNL being involved from table 5 and the number of voxels in the level, we can calculate the probability of each voxel being involved (q), with equation 17.

With the chain and product rule we can calculate the gradient of the objective:

$$\frac{\partial f_{TCP}(d)}{\partial d_j} = -w_{TCP} * \left[\prod_{i=1}^{N_t}\left(1 - q + q * \frac{e^{\frac{d_i - TD50}{\frac{25}{m_{50}}}}}{1 + e^{\frac{d_i - TD50}{\frac{25}{m_{50}}}}}\right)\right] * \left[\sum_{i=1}^{N_t} \frac{\frac{q * e^{\frac{d_j - TD50}{\frac{25}{m_{50}}}}}{k * \left(1 + e^{\frac{d_j * TD50}{\frac{25}{m_{50}}}}\right)^2}}{\left(1 - q + q * \frac{e^{\frac{d_i - TD50}{\frac{25}{m_{50}}}}}{1 + e^{\frac{d_i - TD50}{\frac{25}{m_{50}}}}}\right)}\right] \tag{53}$$

The addition of -1 to the objective requires subtracting the TCP gradient from the other gradients due to the resulting negative sign.
We are left with finding appropriate weightings for the mean objective and TCP objective (w_{TCP}). To get a feeling for an appropriate weight, we looked at the different objective values. The number of voxels included in each objective was not used to normalize the values.

Quadratic objective $= 318.5$

Falloff objective $= 0.0018$

Mean dose objective for PCM $= 0.00028$

By considering the different objective values, we can see that the falloff objective and the mean objective are quite small. Without any weight ($w_{TCP} = 1$) the TCP objective will be between 0.04 and 0. This will be too large, shown in figure 12. The TCP objective completely dominates the mean objective, and there is no tradeoff. A too high TCP objective leads to overdosing the level. The targeted LNL is still part of the PTV 3 and should not receive more than 50 Gy. We decided to try different weights displayed in figure 12. We would like to see the tradeoff between mean dose objective and TCP objective. The closer one gets to the OAR the less dose should be delivered to the LNL.

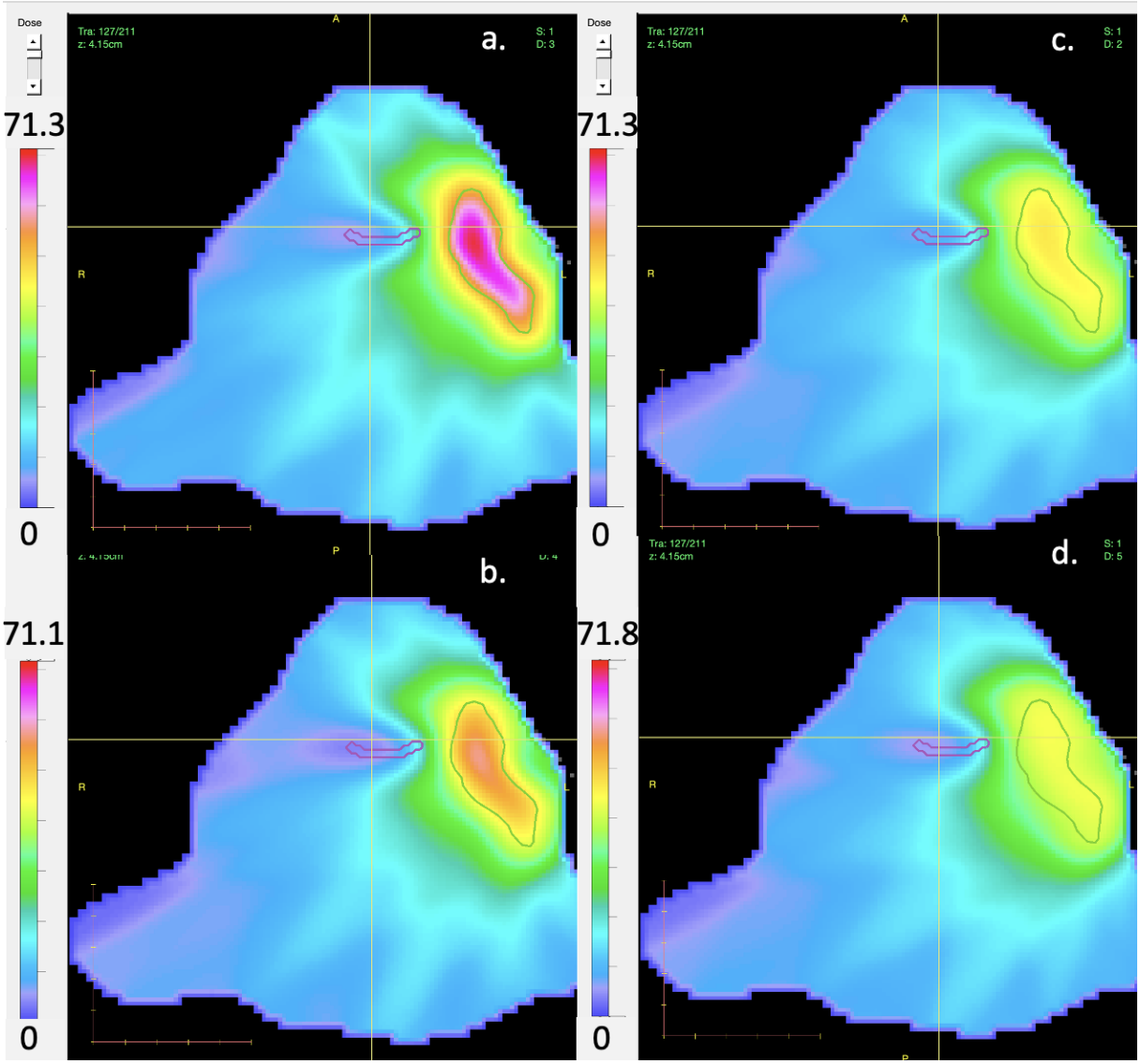

Figure 12: a.) Optimized dose distribution for patient 6 with $w_{PCM} = 1$ and $w_{TCP} = 1$. Contoured are ipsilateral LNL III and the PCM. The TCP objective overpowers the mean objective and greatly overdoses the LNL. b.) For $w_{PCM} = 1$ and $w_{TCP} = 0.2$, there is still an overdosing of the targeted level. c.) With a smaller $w_{TCP} = 0.1$ and a $w_{PCM} = 1$ there is a small trade-off visible. d.) A higher $w_{PCM} = 2$ was tried to see if there is a difference. A bit less dose near PCM.

For each voxel in the targeted LNL, the TCP objective decides how much dose should be delivered. For this patient, the reduction in dose near the OAR is not as clear as we would like. This can have different reasons, most likely it is due to the distance between the LNL and the PCM. To better illustrate the small trade-off, that is achieved, the scaling of the displayed dose is changed in figure 13. The dose displayed is changed such that only 40 to 71 Gy are shown. In this figure, we can see the trade-off between the mean and TCP objective. There is less dose delivered to the LNL where the PCM is near.

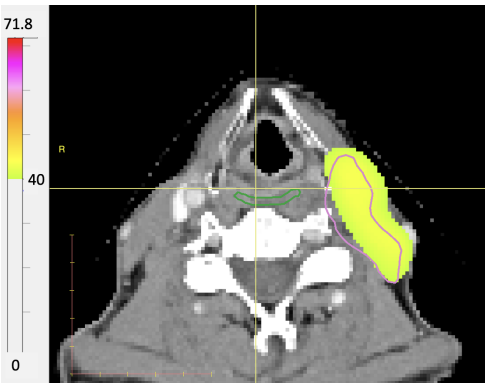

Figure 13: Dose distribution of patient 6 with $w_{PCM} = 2$ and $w_{TCP} = 0.1$ with adapted dose scale.

The non optimal tradeoff between the two objectives is reflected in the NTCP and TCP calculation in table 7. For a better comparison, we also added the NTCP and TCP value without a mean objective and with only a mean objective. Here we can see the improvement from the TCP objective. Improving the NTCP value leads to a reduction in TCP. This small to no improvement can be related to the low probability of LNL III being involved. With the 4% there is only a small range for the TCP objective to move in.

w_{PCM}	w_{TCP}	NTCP dysphagia	TCP
1	1	59.3%	99.8%
1	0.1	59.9%	98.8%
1	0.2	58.4%	99.5%
2	0.1	58.7%	98.5%
0	0	63.9%	99.6%
1	0	59.2%	99.6%

Table 7: NTCP and TCP calculations for patient 6 with different weights for the mean and TCP objective. If $w_{TCP} = 0$ this means that the targeted LNL (ipsilateral III) was included in the quadratic objective for the elective target volume.

5.7 Results

The same procedure described in chapter 5 up to this point is repeated for 3 other patients. Apart form different anatomies, the probabilities of microscopic involvement in the LNL differs. Thus the weights for the mean objective, the TCP objective and the NTCP models are adjusted. The numbering of the patients corresponds to that in table 1. Patients with too large tumors were excluded. We decided to apply the TCP objective to LNL that have a probability between 4% to 10%. Higher probabilities were included in the PTV 3, since the risk of an occult metastasis is too high for a non-conformal treatment. Lower probabilities will most likely not influence the dose distribution, because the room for improvement is small. We applied the TCP objective to LNL II and III. For the other LNL, no suitable patient was available. For each patient we calculated a plan with no mean objective and a mean objective, to be able to compare our plans with the TCP objective to a baseline.

5.7.1 Patient 2

For the second patient, the risks for each LNL was calculated. Judging from the information in table 8 we decided to apply the TCP objective to LNL II on the contralateral side. The

involvement probability of Ipsilateral level III is too low. Two organs are near LNL II, the parotid gland and the submandibular gland. We only considered the contralateral glands for the mean objective. Considering both sides would lead to disturbance of the dose to the target. To reduce the dose to both, we added a mean objective for each organ.

#	**T-stage**	**midline**	**metastases**	**ipsi**	**contra**
2	T2	True	none	II (21%), III (3%)	II (5%)

Table 8: Risk prediction for patient 2 based on the T-stage, midline extension and metastasis. In this case, we would irradiate LNL II on both sides.

Different weights for the submandibular gland, parotid gland and TCP were used. The different dose distributions are displayed in figure 14. Two slices out of the CT images are displayed to show the parotid gland 14a-c and the submandibular glands 14d-f.

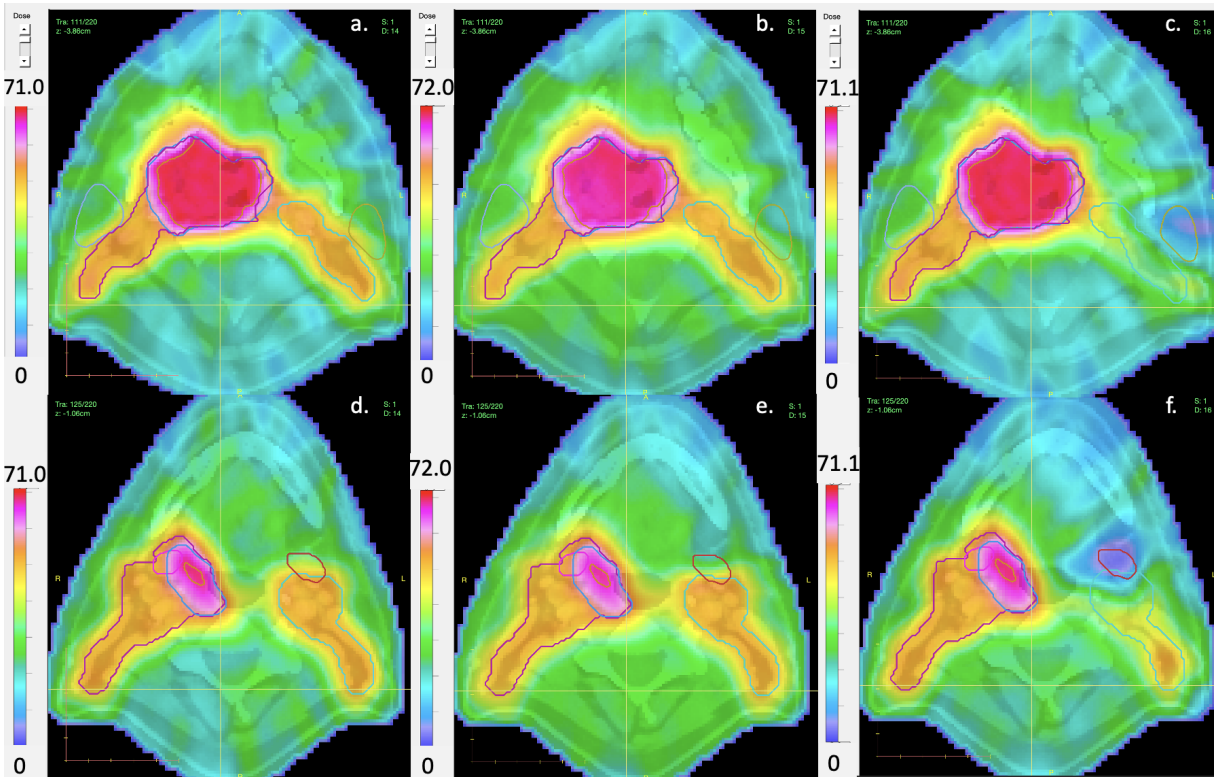

Figure 14: a.-c.) a.)Dose distribution around the parotid gland with quadratic objectives for the three PTVs. b.) A mean objective for the contralateral parotid gland was added. c.) No quadratic objective for LNL II contralateral but the TCP objective is applied to LNL II and mean objective for contralateral parotid gland.
d.-f.) d.) Dose distribution around the submandibular gland, with quadratic objectives for the three PTVs. e.) A mean objective for submandibular gland was added. f.) No quadratic objective for LNL II contralateral but the TCP objective is applied to LNL II and a mean objective for contralateral submandibular gland.

There is a clear trade-off between the TCP and mean objectives. Especially, the trade-off between submandibular gland and dose to the LNL is large. There is clearly less dose delivered to the level where the gland is nearest. The TCP objective delivers the highest dose where the OAR is the furthest away. For further insight, we looked at the TCP and NTCP values.

The two NTCP models we considered are the one that predicts xerostomia (eq. 7) and the one that predicts sticky saliva (eq. 8). For the sticky saliva score that is missing, we assumed a baseline of 1. We did not try to minimize the dose to the sublingual gland, since it is too far away from LNL II and due to the minus factor which means that delivering less dose would lead to a worse result. From patient 6 we have an idea how to set the TCP weight and decided to stick with 0.1. The weights, NTCP and TCP calculations are listed in table 9.

$w_{submanibular}$	$w_{parotid}$	w_{TCP}	**xerostomia**	**Sticky saliva**	**TCP**
1	1	0	60.5%	50.6%	99.4%
1	1	0.1	52.6%	25.8%	97.8%
0	0	0	63.3%	60.3%	99.4%

Table 9: Weights, NTCP and TCP values for patient 2. For $w_{TCP} = 0$ LNL II contralateral was included into the quadratic objective.

There is a clear reduction for the NTCP values, especially for the sticky saliva score. This reduction is possible by losing less than 2% of the tumor control.

5.7.2 Patient 1

Judging from table 10 we decided to use the TCP objective on both LNL III. To apply the TCP model for both levels, a TCP objective for each LNL was added.

#	**T-stage**	**midline**	**metastases**	**new ipsi**	**new contra**
1	T2	True	Ipsi: II, contra: II	II (100%), III (9%)	II (100%), III (5%)

Table 10: Risk prediction for patient 1. The right side is the ipsilateral side, the left side the contralateral.

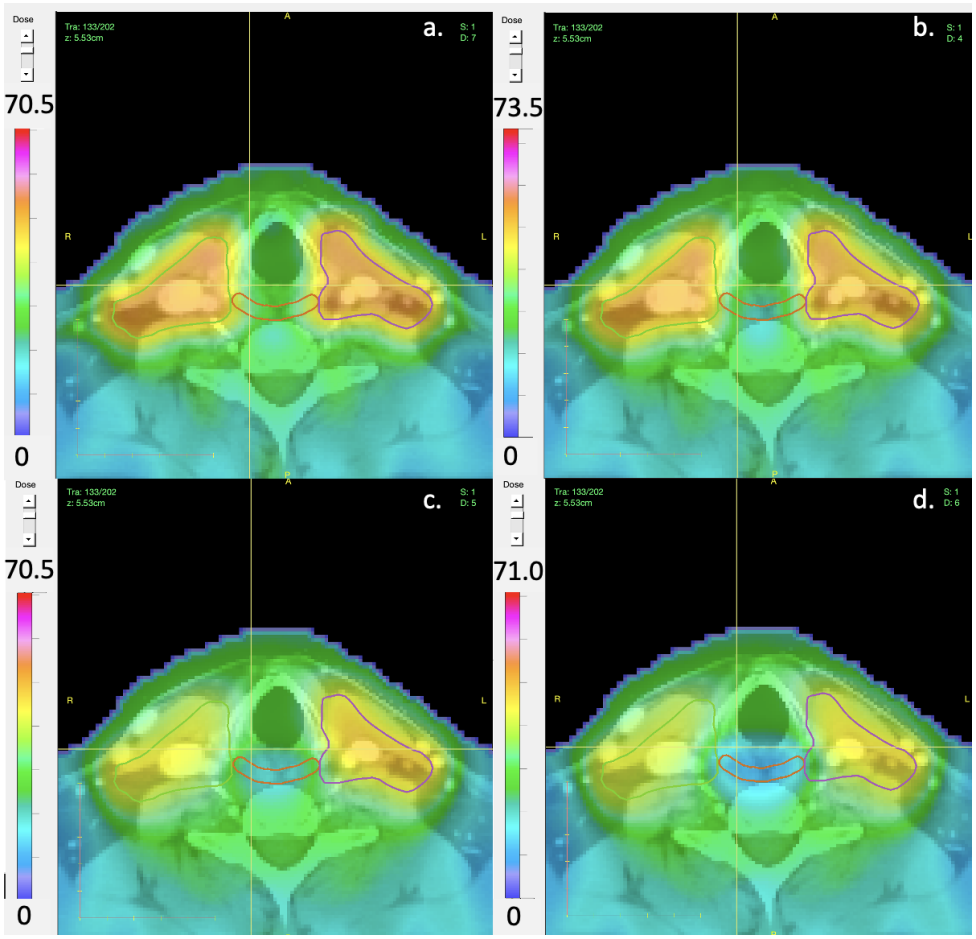

Figure 15: a.) Dose distribution of patient 1 with quadratic objective for both LNL III. Contoured are both LNL III and the PCM. b.) Added mean objective with $w_{pcm} = 1$. c.) Both LNL no longer irradiated with quadratic objectives but now with the TCP objective. TCP weight set to 0.1 and mean weight set to 1. d.) Increased mean weight to 5.

With a mean weight added to the PCM there is a small reduction of dose around said organ. In figure 15 c.) the trade-off between the PCM and the two LNL is visible. By increasing the mean weight, it becomes even more prominent. The optimization delivers less dose near the OAR and increases the dose further away from the structure, while not overdosing the target. Interestingly, it delivers more dose to the contralateral (left) LNL which has a lower involvement probability. For the NTCP calculation, we look at the model that predicts dysphagia from equation 48. The TCP was calculated separately for each LNL due to the different involvement probabilities. The calculations and the weights are listed in table 11.

w_{PCM}	w_{TCP}	NTCP dysphagia	TCP_{contra}	TCP_{ipsi}
1	0.1	50.1%	97.6%	98.2%
5	0.1	42.2%	96.7%	97.9%
0	0	55.5%.	98.9%	99.5%
1	0	53.1%	99.0%	99.3%

Table 11: A list of the different weights for patient 1, with the corresponding NTCP and TCP calculations. For $w_{TCP} = 0$ both LNL III were included into the quadratic objective.

Similar to patient 6 there is no huge reduction in NTCP value with a weight equal to 1. However, even when sparing the PCM the probability of curing the tumor remains high. By increasing

the weight of the mean objective, we can achieve a smaller probability for the side effect while still maintain a high TCP value.

5.7.3 Patient 8

The last patient we looked at is patient 8. We again are using the TCP objective for LNL III. Because we saw in previous patients, that the sparing of the PCM can be quite difficult, we decided to not only spare the PCM but also the thyroid. All the relevant patient and treatment information is given in table 12.

#	**T-stage**	**midline**	**metastases**	**ipsi**	**contra**	**Thyroid volume**
8	T2	False	Ipsi: II	II (100%), III (8%)	none	12.4 cm^3

Table 12: Risk prediction for patient 8. The thyroid volume was added for later NTCP calculations.

The generated dose distributions for patient 8 are shown in figure 16.

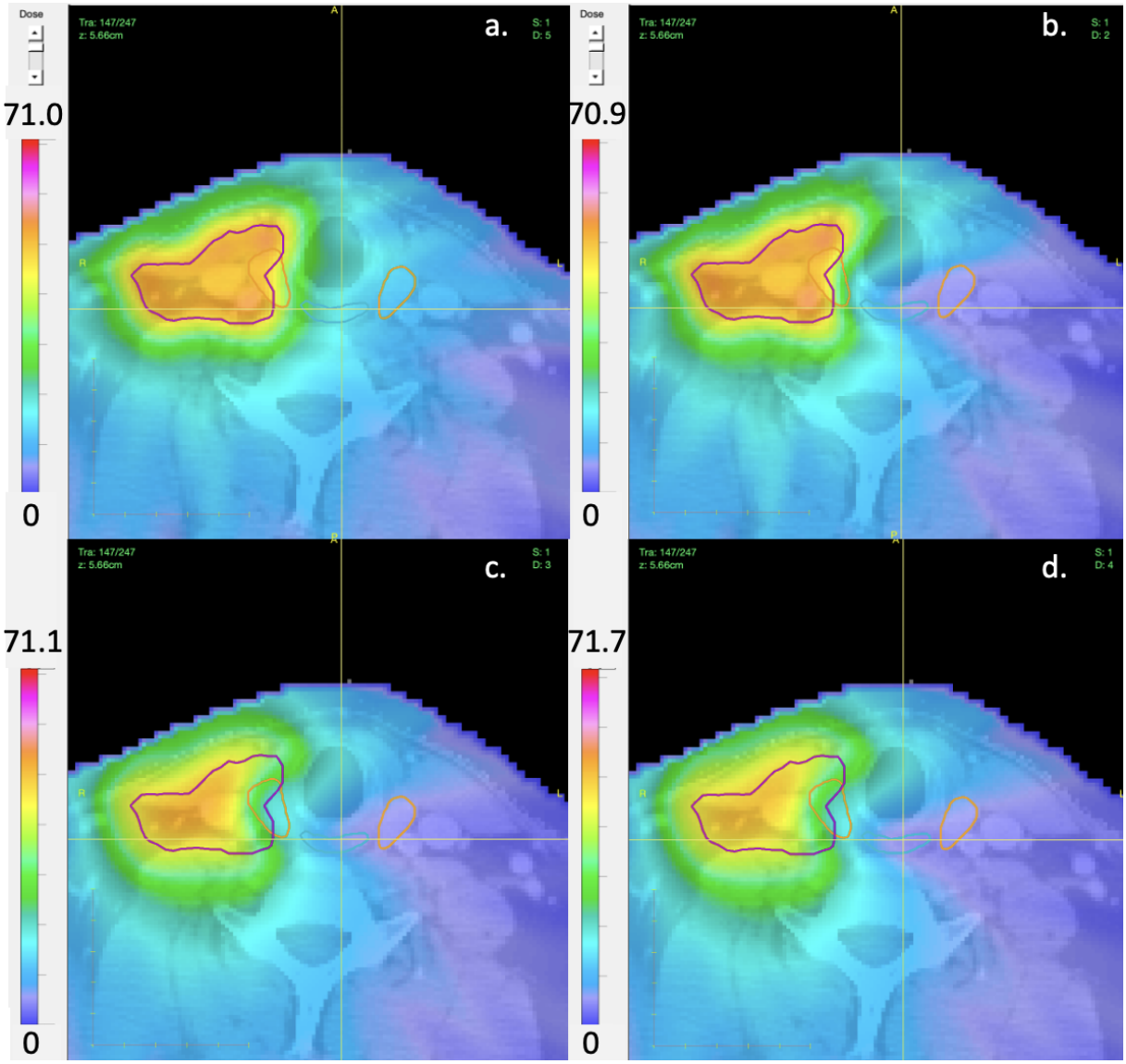

Figure 16: a.) In patient 8 the LNL III ipsilateral, the PCM and the thyroid is contoured. Overlaid with a dose distribution from a quadratic objective for LNL III ipsilateral with no mean objectives. b.) Dose distribution with two mean objectives for PCM and thyroid with weight 1. c.) LNL III no longer is irradiated by quadratic objective but now by TCP objective with weight 0.1 Weights of mean objectives are the same as in picture b. d.) Increased PCM weight to 5.

For this patient, the thyroid structure and the irradiated LNL overlap. By only adding a mean objective to both OAR there are only minor changes because the quadratic objective in the level is stronger. When the TCP objective is added, the mean objective has a higher chance of having an impact. The change in the dose delivered to the PCM is not that large in the lower part of the LNL where also the thyroid is present. Further in cranial direction, the mean objective of the PCM has a higher impact. There the increase in weight to the PCM is clearly visible. With the thyroid overlapping the target, a nice trade-off is achieved. The closer we get to the organ that should be spared, the less dose is delivered.
The exchange between the target and OAR is further shown in the NTCP and TCP calculations in table 13. For the NTCP calculations, we looked at equation 48 and 10.

w_{PCM}	$w_{thyroid}$	w_{TCP}	NTCP dysphagia	NTCP thyroid	TCP
1	1	0.1	28.1%	63.3%	98.2%
5	1	0.1	19.1%	61.0%	97.9%
0	0	0	35.5%	69.0%	99.1%
1	1	0	25.7%	69.0%	99.1%

Table 13: Weights, NTCP and TCP calculations for patient 8. For $w_{TCP} = 0$ LNL III ipsilateral was included into the quadratic objective.

By adding the TCP objective, there is a slight increase in the probability of getting dysphagia, but the chance of hypothyroidism can be reduced. The slight increase could be due to the fact that with the TCP objective a sparing of the overlapping thyroid becomes possible and with that the PCM loses a bit of priority in the optimizations. We increased the weight of the PCM and achieved a large reduction in the NTCP for dysphagia. For Both cases, we were still able to achieve a high tumor control.

For all the treated patients, we were capable to achieve a reduction in the risk of getting side effects, while maintaining a good TCP value. Important to note is that for each case, different weights for the TCP and mean objective were tested. While for the TCP objective a weight of 0.1 is well fitting for all patients, the weights for the OAR had to be determined for each patient. But a weight of 1 overall leads to a good result.

6 Discussion

6.1 Comparing standard care with volume de-escalate treatment plans

Table 1 shows the difference in the elective target volume for standard care and volume de-escalate treatment plans. In standard care the ipsilateral and contralateral side always get irradiated [5]. For an early T-stage and no midline extension, the lymphatic spread model leaves out the whole contralateral side. The levels that have a metastasis are always included in the new plans. Further, we can see that at least on one side LNL II always gets included into the elective target volume. The standard care plan frequently irradiates ipsilateral I-V and adds VII, while on the contra lateral side it includes II-IV. With the new plan, LNL I only gets irradiated if involved. LNL IV is excluded if LNL III is healthy and V is nearly always excluded unless LNL IV is involved. These reductions lead to a smaller target volume and to less dose in the lower areas of the neck.
The dose calculation from table 3 show how the volume de-escalate plans deliver less dose to the lower areas of the neck. Late T-stage patients have less reduction in the lower areas, because LNL III or IV are more often included. In patient 7 and 8 an overall reduction in dose for the considered structures is possible with the de-escalate plan. This is due to the sparing of the contralateral side. Since we do not irradiate LNL I, we should be able to spare the submandibular and sublingual gland. This is not always possible, especially for the late T-stage patients. In these patients, it can happen that the tumor is so large, that parts of LNL I are included into PTV 1 or PTV 2.
With the NTCP calculations, we wanted to quantify these reductions and improvements. In table 4 we see that the biggest dose reductions are achieved in patients 7 and 8. In these patients, every NTCP value was reduced.
Not all NTCP models are equally useful. The models that predict swallowing problems (section 3.1.2) show overall very low probabilities, which is good for the patient but leaves only very little room for improvement. They assign little weight to the dose parameters in their models. Therefore, even though one can significantly reduce the dose to a structure, it has only a small impact on the NTCP value. The swallowing problem models have higher weight for treatment modalities like radiation technique or chemoradiation. These parameters were not changed in our work, such that no improvement could be made.
The NTCP model that shows the most improvement with volume de-escalate plans is the hypothyroidism model. Since we never irradiated LNL V and only in one case LNL IV was included. This reduces the dose to the thyroid greatly, due to the proximity of the two LNL, and with that the NTCP value.
Reducing the probability of sticky saliva and xerostomia is more difficult. sparing the parotid and submandibular glands is only possible if we can spare the contralateral side. Else, LNL II is always included for both sides, which is the LNL right next to the parotid glands. By not irradiating LNL I the sticky saliva score is reduced, but as already mentioned if the tumor is too big, then sparing the submandibular and sublingual glands is only partly possible. The small increases in dose and NTCP values for the de-escalate plans are mostly due to the optimization in Eclipse. The small fluctuations show that the optimization not always took the same path.
In the end we see a reduction in side effects due to reduced volume. But only from these calculations, we can not see if we missed an occult metastasis in a LNL that we did not treat. This question can only be answered by delivering the new treatment plans to actual patients.

6.2 Implementation of a treatment plan optimization

The overall goal of the second part of this thesis was achieved by implementing a voxel based TCP model into a treatment plan optimization to deliver an inhomogeneous dose distribution to the target. We were able to achieve a high TCP value while still reducing the NTCP values for

each patient. We were also capable to take the model from Bortfeld et al. 2021 [20] and extend it to an applicable situation with real patient data. Further, we were able to reduce the size of the subvolumes to the size of a voxel.
In the different dose distributions in chapter 5.6 we can see that with a TCP objective added to the treatment planning process, it can effectively balance the dose distribution between the tumor and the organs at risk by delivering an inhomogeneous dose distribution. To achieve such a trade-off it is important to consider each patient separately. The weights for the mean objective need to be chosen for each patient, while the weight for the TCP objective is optimally set at 0.1. With a TCP weight of 0.1 we have a chance of achieving a balance between NTCP and TCP, while not overdosing the target.
For the mean weight, we noticed that the distance between the OAR and the target matters. If the structure is right next to the target, or even overlaps, then a mean weight of one is appropriate. But for the PCM, where the distance to LNL III is quite big, a higher mean weight was used to achieve a nice trade-off. This can be seen in patient 1, 6 and 8. To achieve a reduction in the dysphagia score, a higher mean weight for the PCM was taken. Optimizing the mean objective for the PCM was challenging, because we always had to cut a part of the PCM out of the mean objective due to its overlap with PTV 1 or PTV 2.
In the different dose distributions, we can clearly see the balance between the TCP objective and the mean objective. The further away the dose distribution is from the structure at risk, the more dose the optimization delivered.
Three (xerostomia, swallowing and tube feeding) out of the 9 NTCP models were used in a different study to decide if a head and neck cancer patient should receive proton or photon therapy. Most patients were selected for proton therapy based on dysphagia related toxicities and had an advanced disease. The patient were selected because the NTCP models showed a great reduction for proton therapy. [28] With our approach, we were able to avoid the higher costs of proton therapy and were still able to reduce the NTCP values in comparison to the standard care plans. In our case the volume reduction was especially dominant for the early T-stage patients. There the biggest impact is visible. With our approach we are able to reduce the NTCP values for oropharyngeal cancer by irradiating less volume with photons.

7 Conclusion and Outlook

In the first part of this work, we have shown how volume de-escalated treatment plans can lower the dose to important OARs which may improve the patient's overall and long term health. With the lymphatic spread model, we can reduce the target volume greatly, especially in lower neck region. By decreasing the size of the elective target volume, we decrease the dose to the healthy tissue. The reduction in the expected side effects were measured with different NTCP models. In this part, the elective target volume was irradiated uniformly.
In the second part, we went from homogeneous to inhomogeneous dose distributions. We delivered inhomogeneous dose distribution to LNL with low probabilities of involvement. We developed a TCP model that takes the probability of each voxel having cancer into account. The probability for each LNL was calculated with the lymphatic spread model. We were able to deliver inhomogeneous dose distribution, where there is less dose delivered near an OAR and a higher dose in the rest of the LNL. Our approach involved the careful balancing of TCP and NTCP values.
In conclusion, this thesis contributes to the field of radiotherapy by providing a real life example of an optimization with TCP objective and showing how volume de-escalate plans could benefit patients.

The NTCP model used were all developed for patient with standard care plan. It would be interesting to look at NTCP models that were developed for volume de-escalated plans, because they would assign different importance to other OAR that are spared with the volume de-escalated plans.
Right now, this optimization runs on a research environment. For further clinical exploration, more work to decrease the computational complexity needs to be done. At this point, the optimization process took an hour, sometimes even longer.
In an additional step, we could consider more flexibility for the probability of each voxel being involved, such that q is no longer the same for all voxels. We could assign different Q for different parts of the target, to better describe the tumor spread. Already visible lymph nodes could have a higher probability. The transition from one LNL to another could be better described with a probability that not just changes at the boarder of two LNL. We could model the probability as a gradient that decreases the further down in the LNL we go.

In the end, the idea of a reduced target volume only makes sense if the prevalence of occult metastasis is predicted right. It makes non sens to deliver radiation to a reduced volume and at the same time have more occurrences of not treated metastasis. To show that the model has accurate predictions, it needs to be tested with real patients. At the moment, such a study is in the works at the University Hospital Zurich. Further, the idea of the reduced target volume and the TCP objective could be applied to other tumor sites than oropharyngeal cancer.

8 Acknowledgement

I would like to thank my supervisor Prof. Dr. Jan Unkelbach for welcoming me into his group at the University Hospital of Zurich in the Department of Radiation Oncology. His inputs, guidance and advice were always useful and had a substantial contribution to this thesis. I am thankful to Yoel Pérez Haas for helping me out when ever I was stuck and explaining new concepts to me.

I would also like to thank Esmée Looman for answering my anatomy and contouring questions. Additionally, I would like to thank Klara Kefer for giving me an introduction into treatment planning with Eclips. I say thank you to the rest of the office for welcoming me and all the nice lunches.

At last, a big thank you goes to my family and friends who supported me during my studies.

References

[1]M. Joiner and A. v. d. Kogel, eds., *Basic clinical radiobiology*, Fifth edition (CRC Press/Taylor & Francis Group, Boca Raton, FL, 2018).

[2]J. Unkelbach, "Khan's treatment planning in radiation oncology", eng, in, edited by F. M. Khan, J. P. Gibbons, and P. W. Sperduto, 4th edition, OCLC: 951081881 (Lippincott Williams & Wilkins, Philadelphia, PA, 2016) Chap. Intensity-Modulated Radiation Therapy: Photons.

[3]A. Barrett, ed., *Practical radiotherapy planning*, 4th ed, OCLC: ocn317748098 (Hodder Arnold, London, 2009), 468 pp.

[4]R. Ludwig, "Modelling lymphatic metastatic progression in head and neck cancer", en, Doktorarbeit (2023).

[5]J. Biau, M. Lapeyre, I. Troussier, W. Budach, J. Giralt, C. Grau, J. Kazmierska, J. A. Langendijk, M. Ozsahin, B. O'Sullivan, J. Bourhis, and V. Grégoire, "Selection of lymph node target volumes for definitive head and neck radiation therapy: a 2019 update", Radiotherapy and Oncology **134**, 1–9 (2019).

[6]R. Ludwig, J.-M. Hoffmann, B. Pouymayou, M. B. Däppen, G. Morand, M. Guckenberger, V. Grégoire, P. Balermpas, and J. Unkelbach, "Detailed patient-individual reporting of lymph node involvement in oropharyngeal squamous cell carcinoma with an online interface", en, Radiotherapy and Oncology **169**, 1–7 (2022).

[7]"A Bayesian network model of lymphatic tumor progression for personalized elective CTV definition in head and neck cancers", **64**, 10.1088/1361-6560/ab2a18.

[8]R. Ludwig, B. Pouymayou, P. Balermpas, and J. Unkelbach, "A hidden Markov model for lymphatic tumor progression in the head and neck", en, Scientific Reports **11**, 12261 (2021).

[9]K. Price, K. M. Van Abel, E. J. Moore, S. H. Patel, M. L. Hinni, A. V. Chintakuntlawar, D. Graner, M. Neben-Wittich, Y. I. Garces, D. L. Price, J. R. Janus, N. R. Foster, B. F. Ginos, R. L. Foote, and D. Ma, "Long-term toxic effects, swallow function, and quality of life on MC1273: a phase 2 study of dose de-escalation for adjuvant chemoradiation in human papillomavirus-positive oropharyngeal cancer", International Journal of Radiation Oncology*Biology*Physics **114**, 256–265 (2022).

[10]S. Gulliford and I. E. Naqa, "Modelling of radiotherapy response (tcp/ntcp)", en, in *Machine and deep learning in oncology, medical physics and radiology*, edited by I. El Naqa and M. J. Murphy (Springer International Publishing, Cham, 2022) Chap. 17.

[11]I. Beetz, C. Schilstra, P. van Luijk, M. E. M. C. Christianen, P. Doornaert, H. P. Bijl, O. Chouvalova, E. R. van den Heuvel, R. J. H. M. Steenbakkers, and J. A. Langendijk, "External validation of three dimensional conformal radiotherapy based NTCP models for patient-rated xerostomia and sticky saliva among patients treated with intensity modulated radiotherapy", Radiotherapy and Oncology **105**, 94–100 (2012).

[12]K. Wopken, H. P. Bijl, A. van der Schaaf, H. P. van der Laan, O. Chouvalova, R. J. H. M. Steenbakkers, P. Doornaert, B. J. Slotman, S. F. Oosting, M. E. M. C. Christianen, B. F. A. M. van der Laan, J. L. N. Roodenburg, C. René Leemans, I. M. Verdonck-de Leeuw, and J. A. Langendijk, "Development of a multivariable normal tissue complication probability (NTCP) model for tube feeding dependence after curative radiotherapy/chemo-radiotherapy in head and neck cancer", Radiotherapy and Oncology **113**, 95–101 (2014).

[13]M. E. M. C. Christianen, C. Schilstra, I. Beetz, C. T. Muijs, O. Chouvalova, F. R. Burlage, P. Doornaert, P. W. Koken, C. R. Leemans, R. N. P. M. Rinkel, M. J. de Bruijn, G. H. de Bock, J. L. N. Roodenburg, B. F. A. M. van der Laan, B. J. Slotman, I. M. Verdonck-de Leeuw, H. P. Bijl, and J. A. Langendijk, "Predictive modelling for swallowing dysfunction after primary (chemo)radiation: results of a prospective observational study", Radiotherapy and Oncology **105**, 107–114 (2012).

[14]M. J. Boomsma, H. P. Bijl, M. E. M. C. Christianen, I. Beetz, O. Chouvalova, R. J. H. M. Steenbakkers, B. F. A. M. van der Laan, B. H. R. Wolffenbuttel, S. F. Oosting, C. Schilstra, and J. A. Langendijk, "A prospective cohort study on radiation-induced hypothyroidism: development of an NTCP model", International Journal of Radiation Oncology*Biology*Physics **84**, e351–e356 (2012).

[15]T. A. Van De Water, H. P. Bijl, H. E. Westerlaan, and J. A. Langendijk, "Delineation guidelines for organs at risk involved in radiation-induced salivary dysfunction and xerostomia", Radiotherapy and Oncology **93**, 545–552 (2009).

[16]M. E. Christianen, J. A. Langendijk, H. E. Westerlaan, T. A. Van De Water, and H. P. Bijl, "Delineation of organs at risk involved in swallowing for radiotherapy treatment planning", Radiotherapy and Oncology **101**, 394–402 (2011).

[17]M. Choi, T. Refaat, M. S. Lester, I. Bacchus, A. W. Rademaker, and B. B. Mittal, "Development of a standardized method for contouring the larynx and its substructures", Radiation Oncology **9**, 285 (2014).

[18]P. Okunieff, D. Morgan, A. Niemierko, and H. D. Suit, "Radiation dose-response of human tumors", International Journal of Radiation Oncology*Biology*Physics **32**, 1227–1237 (1995).

[19]A. Lühr, S. Löck, A. Jakobi, K. Stützer, A. Bandurska-Luque, I. R. Vogelius, W. Enghardt, M. Baumann, and M. Krause, "Modeling tumor control probability for spatially inhomogeneous risk of failure based on clinical outcome data", en, Zeitschrift für Medizinische Physik **27**, 285–299 (2017).

[20]T. Bortfeld, N. Shusharina, and D. Craft, "Probabilistic definition of the clinical target volume—implications for tumor control probability modeling and optimization", Physics in Medicine & Biology **66**, Publisher: IOP Publishing, 01NT01 (2021).

[21]P. C. Hansen, V. Pereyra, and G. Scherer, *The linear data fitting problem*, eng (Johns Hopkins University Press, Baltimore, Md, 2013) Chap. 1.

[22]S. Das, "A brief note on estimates of binomial coefficients",

[23]J. O. Deasy, A. I. Blanco, and V. H. Clark, "CERR: A computational environment for radiotherapy research", en, Medical Physics **30**, 979–985 (2003).

[24]A. Wächter and L. T. Biegler, "On the implementation of an interior-point filter line-search algorithm for large-scale nonlinear programming", en, Mathematical Programming **106**, 25–57 (2006).

[25]J. Unkelbach and D. Papp, "The emergence of nonuniform spatiotemporal fractionation schemes within the standard BED model", en, Medical Physics **42**, 2234–2241 (2015).

[26]T. Kanehira, S. Van Kranen, T. Jansen, O. Hamming-Vrieze, A. Al-Mamgani, and J.-J. Sonke, "Comparisons of normal tissue complication probability models derived from planned and delivered dose for head and neck cancer patients", Radiotherapy and Oncology **164**, 209–215 (2021).

[27]S. A. Bhide, S. Gulliford, U. Schick, A. Miah, S. Zaidi, K. Newbold, C. M. Nutting, and K. J. Harrington, "Dose–response analysis of acute oral mucositis and pharyngeal dysphagia in patients receiving induction chemotherapy followed by concomitant chemo-IMRT for head and neck cancer", Radiotherapy and Oncology **103**, 88–91 (2012).

[28]M. Tambas, R. J. H. M. Steenbakkers, H. P. van der Laan, A. M. Wolters, R. G. J. Kierkels, D. Scandurra, E. W. Korevaar, E. Oldehinkel, T. W. H. van Zon-Meijer, S. Both, J. G. M. van den Hoek, and J. A. Langendijk, "First experience with model-based selection of head and neck cancer patients for proton therapy", Radiotherapy and Oncology **151**, 206–213 (2020).